

©2020

John El-khour

ALL RIGHTS RESERVED

FLEXURAL BEHAVIOR OF SIMPLY SUPPORTED CONCRETE BEAMS PRESTRESSED  
WITH STEEL AND FRP TENDONS

By

JOHN EL-KHOURI

A thesis submitted to the

School of Graduate Studies

Rutgers, The State University of New Jersey

In partial fulfillment of the requirements

For the degree of

Master of Science

Graduate Program in Civil and Environmental Engineering

Written under the direction of

Hani H. Nassif

And approved by

---

---

---

New Brunswick, New Jersey

January 2020

# **ABSTRACT OF THE THESIS**

## **FLEXURAL BEHAVIOR OF SIMPLY SUPPORTED CONCRETE BEAMS PRESTRESSED WITH STEEL AND FRP TENDONS**

By JOHN EL-KHOURI

Thesis Director:

Dr. Hani H. Nassif

Unbonded tendons are being applied more often in the strengthening and rehabilitation of current deteriorated concrete structures. The use of unbonded steel tendons without any protective material presents a higher risk for corrosion. Therefore, unbonded CFRP tendons can be applied in lieu of or in combination with steel tendons due to its high strength and corrosion resistance. This research involves the testing of seven High Performance Concrete (HPC) beams with bonded and unbonded (hybrid) tendons using a combination of steel and CFRP tendons. Several parameters include the area of the unbonded tendons, unbonded tendons material (CFRP or Steel), and depth of unbonded tendons. The experimental testing results in this study includes deflection at mid-span, ultimate load capacity, stress and strain in steel reinforcement, tendons, and concrete, number of cracks, and crack width and spacing for all beams. Finite element analysis for all hybrid beam ultimate strength and deflections are presented and compared to the experimental results. Comparisons of the ultimate stress ( $f_{ps}$ ) in the tendons

between the experimental results with three code equations are presented. Test results show that the use of CFRP as an unbonded tendon in hybrid girders can maintain the same ductility level steel tendon can achieve. Additionally, the finite element analysis predicted a similar behavior of concrete beams prestressed with hybrid tendons.



## ACKNOWLEDGEMENTS

I would like to thank my advisor, Dr. Hani Nassif, for giving me the opportunity to work with him on this research. I also appreciate his guidance and support in this thesis and throughout my graduate degree.

Furthermore, I would like to thank my thesis committee members Dr. Nicole Fahrenfeld and Dr. Adi Abu-Obeidah. I would also like to acknowledge Dr. Abu-Obeidah for his guidance and support in answering any questions I had with my research topic.

I also must thank all of my colleagues and coworkers: Andrew Shehata, Mina Habib, Jonathon Rodriguez, Daniel Okechukwu, Wassim Nasreddine, Albert Hajj Moussa, Alain Hajj Moussa, Harold Castaneda, Pascal El-khoury, and Emily Pooley for helping me with batching, mixing, and testing the beams.

Finally, I would also like thank my family and friends for their love and support throughout my academic career.

# TABLE OF CONTENTS

ABSTRACT OF THE THESIS .....	ii
ACKNOWLEDGEMENTS.....	iv
TABLE OF CONTENTS.....	v
LIST OF FIGURES .....	vii
LIST OF TABLES.....	ix
1. INTRODUCTION .....	1
1.1 Overview.....	1
1.2 Problem Statement.....	2
1.3 Research Objective .....	2
1.4 Structure of the Thesis .....	3
2. LITERATURE REVIEW .....	4
2.1 Introduction.....	4
2.2 Related Investigations.....	5
2.2.1 Prestressing with Unbonded Tendons.....	6
2.2.2 Prestressing with Unbonded and Bonded Tendons .....	10
2.2.3 Anchorage Systems for the CFRP Tendons.....	12
2.3 Cost Benefits Using CFRP Tendons.....	13
2.4 Code Provisions .....	14
3. EXPERIMENTAL PROGRAM.....	16
3.1 Introduction.....	16
3.2 Mechanical Properties Test.....	17
3.2.1 High Performance Concrete.....	17
3.2.2 Prestressing Steel .....	19
3.2.3 Steel Rebar .....	19
3.2.4 CFRP Tendons .....	21
3.3 Casting Process .....	22
3.4 Testing Process .....	27
4. TEST RESULTS.....	30
4.1 Introduction.....	30
4.2 Cracking Behavior .....	30
4.3 Load – Deformation Behavior .....	37
4.3.1 Load – Deflection Relationship .....	37
4.3.2 Load – Strain Relationship.....	46
4.3.3 Stress and Strain in Prestressing Steel and CFRP Tendons.....	56
5. MODELING AND ANALYSIS.....	61
5.1 Introduction.....	61
5.2 Trussed Beam Analogy.....	61
5.2.1 Finite Element Analysis (FEA).....	61
6. COMPARISON OF RESULTS .....	65

6.1	Introduction.....	65
6.1.1	Comparison with the FEM Analysis.....	65
6.1.2	Comparison with the Design Codes.....	67
7.	Conclusions.....	69
	Bibliography .....	71

# LIST OF FIGURES

Figure 3.1 Tensile Testing of Steel Tendon.....	19
Figure 3.2 Tensile Testing of #2 Steel Rebar .....	20
Figure 3.3 Tensile Testing of #3 Steel Rebar .....	20
Figure 3.4 Casting preparations (a) steel cage in the wooden mold, (b) strain gauges installed on multiple locations on the steel cage.....	22
Figure 3.5 Casting process (a) casting concrete in wooden mold, (b) concrete vibrated and leveled .....	24
Figure 3.6 Beam design and cross section details.....	25
Figure 3.7 Beam testing setup.....	27
Figure 3.8 Location of sensors used during beam testing.....	28
Figure 4.1 Crack mapping during beam testing.....	31
Figure 4.2 Cracking Performance of Beams with Steel Tendons.....	33
Figure 4.3 Cracking Performance of Beams with CFRP Tendons .....	34
Figure 4.4 Tendon Area, Depth, and Material Effect on Crack Width.....	35
Figure 4.5 Load-deflection behavior of all prestressed concrete beams tested .....	42
Figure 4.6 Effect of the hybrid combination compared to fully bonded steel tendons on the load-deflection behavior .....	43
Figure 4.7 Effect of the area of the unbonded tendons on the load-deflection behavior at the same depth.....	44
Figure 4.8 Effect of the unbonded tendons depth on the load-deflection behavior .....	45
Figure 4.9 Hybrid beam showing LVDT's at mid-span profile for strain profile measurement .....	46
Figure 4.10 Load-strain behavior of the steel rebar strain for all prestressed concrete beams tested.....	48
Figure 4.11 Load-strain behavior of the steel rebar strain for the hybrid combination compared to fully bonded steel tendons.....	49
Figure 4.12 Effect of the area of the unbonded tendons at the same depth on the load-strain behavior of the steel rebar strain .....	50
Figure 4.13 Effect of the unbonded tendons depth on the load-strain behavior of the steel rebar strain .....	51
Figure 4.14 Load-strain behavior of the bonded tendon strain for all prestressed concrete beams tested.....	52

Figure 4.15 Load-strain behavior of the bonded tendon strain for the hybrid combination compared to fully bonded steel tendons.....	53
Figure 4.16 Effect of the area of the unbonded tendons at the same depth on the load-strain behavior of the bonded tendon strain.....	54
Figure 4.17 Effect of the unbonded tendons depth on the load-strain behavior of the bonded tendon strain.....	55
Figure 4.18 Load-strain behavior of the top tendon strain for all prestressed concrete beams tested.....	57
Figure 4.19 Load-strain behavior of the top tendon strain for the hybrid combination compared to fully bonded steel tendons.....	58
Figure 4.20 Effect of the area of the unbonded tendons at the same depth on the load-strain behavior of the top tendon strain.....	59
Figure 4.21 Effect of the unbonded tendons depth on the load-strain behavior of the top tendon strain.....	60
Figure 5.1 Trussed Beam Model (Nassif, et al., 2003) (Unal, 2011).....	62
Figure 5.2 Concrete Failure Surface in Plane Stress (ABAQUS, 2016) .....	63
Figure 5.3 Tension Stiffening Model (ABAQUS, 2016).....	64
Figure 6.1 Applied Load and Deflections Behavior for All Hybrid Beams: Experimental vs FEM.....	66

# LIST OF TABLES

Table 2.1 Approximate values of $f_{ps}$ at nominal flexural strength for unbonded tendons, (ACI 318-18).....	14
Table 3.1 Mix Design Properties .....	18
Table 3.2 Concrete Mechanical Properties .....	18
Table 3.3 Mechanical Properties of Steel Rebars .....	21
Table 3.4 Mechanical Properties of CFRP Tendons (Tokyo Rope) .....	21
Table 3.5 Summary of the beam properties and parameters.....	26
Table 3.6 Overview and description of sensors used during testing.....	29
Table 4.1 Summary of Crack Spacings, Number, and Widths .....	36
Table 4.2 Tendon Area Effect on Applied Load at the same Crack Width Limit specified by ACI 224.....	36
Table 4.3 Tendon Depth Effect on Applied Load at the same Crack Width.....	36
Table 4.4 Summary of applied loads and measured mid-span deflections at various limit states.....	41
Table 4.5 Measured compressive strain in concrete at extreme top fiber at failure load .	47
Table 4.6 Summary of the effective stress and ultimate stress for the top tendons .....	56
Table 6.1 Summary of the Load Deflection at Ultimate for Hybrid Beams (EXP vs FEM) .....	67
Table 6.2 Summary of the Unbonded $f_{ps}$ for Hybrid Beams (EXP vs Code Equations) ..	68

# CHAPTER I

## 1. INTRODUCTION

### 1.1 Overview

Prestressed concrete has been broadly utilized in many structural projects throughout the years. The use of prestressed concrete has several advantages over regular reinforced concrete. When incorporating prestressing in structural members, longer spans, smaller sections, less deflection, and less cracks can be accomplished as compared to regular reinforced concrete members.

There are two common types of prestressing, pre-tensioning and post-tensioning. In pre-tensioning, the tendons are tensioned in a prestressing bed before casting the concrete and then released from the prestressing bed after the concrete is casted and hardened. The tensile stresses released from the tendons are transferred to the concrete by a full bond as compression. Pre-tensioning is commonly done at factories and applied to smaller sections, which could be easily transported to construction sites. In post-tensioning, the tendons are tensioned after the concrete has been casted and hardened through a duct. Post-tensioning can be performed by either using internal bonded tendons or external unbonded tendons. Bonded tendons are placed inside a duct, tensioned, and then grouted to keep the tendons from corroding. In unbonded tendons, corrosion is prevented by encasing the tendons with grease.

Using a hybrid of bonded and unbonded tendons can benefit in obtaining higher strength and longer clear spans without increasing the depth in a member. With the improvement in recent prestressing techniques for corrosion protection, and the use of

carbon fiber tendons and steel tendons, the use of unbonded tendons is becoming more desirable (Ozkul 2007). Furthermore, the use of bonded steel tendons with unbonded CFRP tendons can improve the strength and ductility of the member (Abu-Obeidah 2017).

## **1.2 Problem Statement**

A substantial amount of prestressed concrete structures are deteriorating and coming to an end of their design life. Many concrete structures are showing large cracks and facing corrosion of the steel reinforcement and steel tendons. One of the many reasons for the causes of cracking on a bridge is the increase in live loads and overloading of trucks. The presence of cracks will allow moisture to seep into the concrete and accelerate the corrosion process in steel. This will damage the steel tendons and decrease its flexural capacity. In order to combat this issue, carbon fiber reinforced polymer (CFRP) tendons can be introduced to replace the use of steel tendons. CFRP tendons are beneficial because of its high strength and corrosion resistance. Several researchers investigated the performance post-tensioning CFRP tendons such as Abu-Obeidah (2017), Jerret et al. (1996) and Burningham et al. (2014). These authors ultimately found that the use of CFRP tendons performed well and increased the ultimate strength and flexural capacity of the beams.

## **1.3 Research Objective**

The objective of this experiment is to observe the flexural behavior of seven prestressed concrete T-beams using a hybrid of bonded and unbonded tendons with steel and CFRP tendons. A comparison of the experimental results with a finite element model and existing equations will be discussed.



## 1.4 Structure of the Thesis

Chapter I describes a general overview of the problem, problem statement, and objectives of this experimental study.

Chapter II is the literature review which includes the existing experimental and analytical investigations on the ultimate stress in unbonded tendons in beams prestressed with unbonded and hybrid tendons. A summary of the different anchorage systems used for CFRP and prediction equations for  $f_{ps}$  used by various Codes will be covered. Furthermore, the cost benefits of using CFRP tendons will be discussed.

Chapter III covers the experimental program, containing all material properties, test parameters, test set-up and arrangement of beams.

Chapter IV presents the results from the experimental study including number of cracks, deflection at mid-span, stress and strain in prestressing strand, reinforcing steel, and concrete. Test results including stress increase in tendon; moments at cracking, at yielding of non-prestressed, at yielding of prestressed steel and at ultimate load, modes of failure, strain in concrete and steel, and deflections are also reported. Finally, the general behavior of beams, both at serviceability and ultimate limit states, and observations pertaining to test results are discussed.

Chapter V presents the analytical formulation of the trussed-beam model at both elastic and inelastic limit states. First presented is a finite element solution using ABAQUS (2016). Then, a global solution to beams prestressed with unbonded and/or bonded tendons is presented.

Finally, Chapter VI summarizes the current investigation, highlights the findings of this research and proposes recommendations.

## **CHAPTER II**

### **2. LITERATURE REVIEW**

#### **2.1 Introduction**

Concrete structures around the world require strengthening to compensate for the damage during their service life. These structures are susceptible to various environmental conditions including, but not limited to, impact loads, corrosion, chemical damage, and erosion. These factors have contributed to the global deterioration of bridges. Although costly, the maintenance and repair of bridges is essential in increasing its design life. The increase in live loads on buildings, and traffic loads on bridges, require reconstructing and rehabilitation in order to maintain the safety of these structures (Shahrooz et al., 2002).

Prestressed concrete members can improve the load bearing capacity of the concrete. The strength of bridges is affected by two key issues: an increase in live load, and corrosion of steel reinforcement. Throughout the years, different approaches have been useful in improving the load bearing capacity of concrete bridges. Unbonded tendons have become a widespread use in strengthening and reconstruction.

The Maine Department of Transportation Bridge Program utilized Carbon Fiber Composite Cables (CFCC) for post-tensioning a voided slab bridge. Maine's coastal environment and harsh winters has a big impact on the corrosion of steel reinforcement. Therefore, the steel tendons were replaced by CFCC tendons to help solve the corrosion issue of the tendons. It was recorded that the redesign and application of CFCC tendons increased the bridge costs by 12%, however, the long-term maintenance costs should be

reduced. Overall, the use of the CFCC tendons were successfully installed and the bridge was successfully rehabilitated (Thompson and Parlin 2013). Furthermore, an inspection on the Midway bridge in Florida indicated corrosion in many cables. The Florida Department of Transportation Structural Research Center was requested to test these corroded cables to discover the remaining tensile capacity of the reinforcement. The test results indicated that the tendons ultimate tensile strength reduced from 279 ksi to an average value of 248 ksi from corrosion.

Unbonded CFRP tendons should be used in order to combat the corrosion problem. Furthermore, CFRP tendons are lighter, more flexible, and have a higher tensile strength capacity and tensile fatigue resistance than steel. This study examines the behavior of prestressed concrete beams with bonded and unbonded tendons using different tendon materials such as steel and CFRP.

## **2.2 Related Investigations**

An experimental study that involved the testing of 25 high strength simply supported beams, which were post-tensioned with unbonded steel tendons, was performed by Ozkul et al. (2008). All beams were prestressed using a straight tendon profile and tested under a three point loading system. Multiple parameters were considered, such as the flexural reinforcing steel area, prestressing steel area, effective prestressing stress, strength of concrete, and span-depth ratio. The testing results were used to confirm a developed analytical model to evaluate the overall beam behavior with unbonded tendons. A finite element analysis software was used to confirm the model for the tested beams. Based on the analytical study, an equation for predicting the stress at

ultimate was derived. When compared to the experimental results, the finite element analysis model and the proposed equation predicted stresses precisely.

The equation developed by Ozkul et al. (2008) was extended by Unal (2011) to include prestressed beams using a hybrid of bonded and unbonded tendons with steel or CFRP tendons. The suggested equation was developed using the Generalized Incremental Analysis (GIA) that applies the trussed beam method developed by Nassif et al. (2003). The predicted equation was demonstrated with 199 beams, which are presented in the literature. The equations were shown in terms of  $e_{psU}$  and  $d_{psU-c}$ . The results showed that all of the proposed equations are precise, however, the equations in terms of  $e_{psU}$  are preferable because they are more accurate when all beams are considered.

### **2.2.1 Prestressing with Unbonded Tendons**

An experimental study was conducted by Bennitz et al. (2012) observing the behavior of seven prestressed concrete beams with unbonded external CFRP tendons. The tendons were anchored using a newly developed anchorage and post-tensioning system. The effects of altering the force of prestressing, tendon depth, and occurrence of a deviator were considered. The testing results indicated that the steel tendons and CFRP tendons experienced similar effects on the performance of the strengthened beams. A model developed by Tan and Ng (1997) was used to predict the beam behavior. The model typically overvalued the beams' capacities and projected higher yield loads than were measured for most beams. Also, the beams' ultimate capacities and ductility was significantly overestimated by the model in the majority of the cases. Tan and Ng (1997) concluded that although the model is useful, it needs to be refined.

Hussien et al. (2012) conducted an experimental study involving the use of prestressed bonded and unbonded steel tendons with normal strength and high strength concrete beams. A total of nine beams were tested; two of which were reinforced with non-prestressed reinforcement, four beams were reinforced with bonded tendons, and the final three beams were reinforced with unbonded tendons. These beams were tested to failure under cyclic loading in order to observe the flexural behavior. The main parameters in this experimental study are the compressive strength (43, 72 and 97 MPa), bonded and unbonded tendons and the prestressing index (0%, 70% and 100%). From the analysis of the test results, Hussien et al. (2012) determined that the beams which were partially prestressed with bonded tendons showed better behavior than those with unbonded tendons. A 265% increase in ductility, 13% initial stiffness and 199% increase in the ultimate deflection was observed between the bonded and unbonded tendons. Furthermore, the authors predicted the ultimate prestressing stress in unbonded tendons using the ACI 423.7-07 and Lee (1999) equations to be up to 95% accurate.

An experimental program of seven simply supported concrete beams, four rectangular and three T-section, post-tensioned with straight unbonded CFRP tendons was investigated by Heo et al. (2012). Several variables were considered to examine the effects of the prestressing reinforcement ratio, the extent of the prestressing force, the type of loading, and the sectional shape on the flexural behavior of the beams. Results showed there was an increase in ductility for beams prestressed with unbonded CFRP tendons than beams prestressed with bonded CFRP tendons. In this research, the ductility of the beams was analyzed based on the energy ratio up to the peak load ( $\mu_p$ ) (Grace and Abdel-Sayed 1998).

A numerical model using the finite element method to predict the complete nonlinear response of five prestressed continuous beams with internal unbonded tendons was developed by Lou et al. (2013). The geometric and material nonlinearities are considered in the model. At any deformed state, the strain increment in unbonded tendon is computed from the extension of the full tendon between end anchorages. The finite element design is created using the layered Euler-Bernoulli beam theory. The strain increment in the tendon is calculated from the elongation of the whole tendon between end anchorages. To acquire the current total strain, prestressing force, and tendon stress, the strain increment is added to the reference strain. When comparing the computational and experimental results, the numerical analysis generates a good load–deflection response from the experimental study. Also, the increase in stress of the unbonded tendons during testing until failure showed good results as well.

Ghallab (2014) tested nine continuous concrete beams to examine the effect of numerous parameters on the ductility of continuous reinforced concrete beams externally strengthened with Parafil ropes. The parameters contained external prestressing force value, external prestressing tendons depth, loading pattern, tendon profile and deviator locations. The author concluded that the reduction in ductility is considerably affected by the increase of effective depth of the prestressing force, the location of deviators and the tendon profile. When the depth of the external prestressing force was increased, crack propagation was reduced, beam stiffness after cracking was better, and the ductility reduced. Therefore, to prevent brittle failure, the tendon depth should be limited. The load pattern before cracking had nearly no effect on the ductility and the stiffness of the beam. However, the load pattern at ultimate had higher ductility at the third span. Finally,

the ductility and cracking pattern of the strengthened beam was improved by changing the location of deviators.

An experimental and analytical study for observing the nominal moment capacity of post-tensioned unbonded members was conducted by El Meski and Harajli (2014). These members were strengthened using external FRP tendons. The experimental program consisted of 36 simply supported samples that were tested to failure. The variables in this program consisted of the internal tension reinforcement area, external FRP reinforcement area, member span-depth ratio, prestressing tendon profile, and the concrete structural system type. The analytical study presented a design-oriented process for calculating the nominal moment capacity of the unbonded post-tensioned FRP specimens with internal or external tendon systems. This process is consistent with the method suggested in ACI Committee 440 report for reinforced concrete or bonded prestressed concrete specimens and is valid for simply supported and continuous members. The experimental test results were used to verify the accuracy of the design approach. The author concluded that using external FRP reinforcement is as successful in improving the nominal flexural strength of unbonded prestressed concrete members, as when used for strengthening bonded prestressed concrete or reinforced concrete members.

A procedure for computing the stress in post-tensioned unbonded continuous beams was conducted by Zhou and Zheng (2014). Sixteen beams were tested and analyzed under static loading up to failure. The key variables in this study are the reinforcement index, the tensioning stress, span-depth ratio, and the effective prestress for the beams. The model was originated from the equilibrium of the ultimate flexural

capacity and was calibrated by the testing data. The proposed equation to predict the stress increase at ultimate of the unbonded tendon is shown in equation 2.1. The equation was found to provide better accuracy for predicting the ultimate stress of the unbonded tendons when compared with the ACI code and China specification. The rotation of plastic hinges and the non-prestressed reinforcement steel are not considered in the ACI 318-08 equation. Also, the effect of plastic hinges is not considered in the China specification equation.

$$\Delta\sigma_{pu} = k_1 k_2 \left( \frac{0.0474}{\beta_p} - \frac{\beta_o}{\beta_p} + 1.7214 \right) \sigma_{pe} \quad (2.1)$$

The casting and testing of three precast segmental concrete T-beams with unbonded steel and CFRP tendons was performed by Pham et al. (2018). The beams have a height and length of 400 mm and 3900 mm, respectively. The joints utilized were either epoxied or dry shear-keyed. Results showed that beams with CFRP tendons can achieve high strength and ductility as compared to beams with steel tendons on precast segmental bridge beams. The type of joints used greatly affected the performance of the beams. Whether steel or CFRP tendons were used, the beams with dry joints presented a similar behavior up to ultimate. However, the beam prestressed with CFRP with epoxied joints deformed linearly until failure after cracking.

### **2.2.2 Prestressing with Unbonded and Bonded Tendons**

Abu-Obeidah (2017) investigated the testing of 15 high strength concrete beams prestressed with bonded and unbonded tendons. Several parameters were considered such



as: the tendon depth, bonded tendon area, unbonded tendon area and material, effective prestress, and span to depth ratio. The author determined that using CFRP as an unbonded tendon can increase the ductility of the member in terms of spacing, width and number of cracks as compared to a steel tendon with the same area.

Tests were conducted on four prestressed concrete beams pre-tensioned with steel tendons and strengthened by exterior CFRP post-tensioned tendons by Jerret et al. (1996). Two CFRP tendons with 8 mm in diameter, harped 4.8 degrees at each of two points were provided. These tendons were externally post-tensioned for strengthening. The beam's effective steel prestress varied from 985 to 1130 MPa. The CFRP tendons post-tensioning stress ranged from 1240 to 1500 MPa. For the CFRP strengthened members, the average strength increase was 115% and 46% for beams with one steel strand two steel strands, respectively. The midspan deflections at ultimate load for strengthened beams were about 60% of the corresponding control beam deflection.

Ghallab and Beeby (2001) tested four prestressed concrete beams to failure in order to observe the advantage of external prestressing using Parafil rope. Of the four beams, one is internally prestressed with steel only and three are internally prestressed with steel but strengthened with external Parafil ropes. The authors concluded that providing external prestressing force improves the stiffness, cracking and ultimate flexural strength without any severe reduction in ductility. Also, prestressing externally can be used to improve beam deflections and regulate cracking.

Burningham et al. (2014) conducted an experimental study testing three prestressed concrete beams. One of the beams was used as a control beam and the other two beams were damaged and post-tensioned with CFRP tendons. The damaged beams

involved the cracking of concrete, and steel tendons that were cut to simulate corrosion and vehicle collision. Beams RP1 and RP3 presented an increase in ultimate strength of 20.6% and 31.1%, respectively. This is with respect to the damaged condition. The increase in ultimate strength of repaired beams, RP1 and RP3, compared to control beam, P2, shows that external post-tensioned CFRP tendons can make up for partial or complete removal of a prestressing strand. Also, it was observed that the damaged beams that were repaired were as ductile as the control beams. This experimental program applies CFRP tendons as a strengthening component for pre-tensioned beams.

### **2.2.3 Anchorage Systems for the CFRP Tendons**

An evaluation of several FRP tendon anchor systems to be used in prestressed concrete structures was conducted by Nanni et al. (1996). A total of ten FRP tendon anchor systems were tested in tension up to failure. These anchors can be separated into three groups: wedge, resin/grout potted, and spike anchors. It was determined that out of the ten anchorage systems, only four systems were successful in terms of being in good agreement with the manufacturers' values of strength, modulus of elasticity, and ultimate strain. The experimental data for the other systems achieved below the manufacturers' values. The resin/grout system developed by Tokyo Rope and Toho Rayon Co. was one of the successful systems tested and will be used in this research.

A bond-type anchorage system using cement-based grout for the use of CFRP tendons was proposed by Zhang and Benmokrane (2004). The anchorage system involves the use of a steel tube where the CFRP tendons are inserted in the tube and then grouted with cement-based grout. The steel tube is threaded on the inside to increase bond strength. Different development lengths of 250, 300, and 500 mm were tested in

monotonic tensioning to examine the bond stress distribution and critical bond length. A multi-rod of 9 CFRP tendons with a development length of 400 mm was tested and achieved at least 90% of the tensile strength. This showed an acceptable tensile behavior for each loading stage investigated.

Schmidt et al. (2010) developed a two-piece wedge anchorage system for CFRP tendons with an combined sleeve and a differential angle among the wedge sections and barrel. The wedge had three slits cut into it. One of the slits was cut open and the other two slits were stopped 1 mm from the inner wedge hole. The sleeve grips the wedge's sections while presetting and loading allowing the CFRP tendon to be held in place. The final anchorage was constructed based on observing the failure modes of previous tests. Overall, the anchorage design was a success as it reached the full capacity of the CFRP tendon and guaranteed a stable load of fracture.

### **2.3 Cost Benefits Using CFRP Tendons**

Eamon et al. (2012) discussed a life-cycle cost analysis (LCCA) of prestressed concrete bridges using CFRP tendons and bars. The variables included the beam type, span length, and the traffic volume. The results indicated that CFRP reinforced bridges can be more cost effective than steel reinforced bridges. A probabilistic analysis was performed and indicated over 95% probability that a bridge reinforced with CFRP will be cheaper between 20 and 40 years of service, which depends on traffic volume and bridge geometry.

A Life Cycle Cost (LCC) of prestressed concrete and FRP footbridges was calculated by Nishizaki et al. (2006). This study considered the use of an existing FRP footbridge constructed in Okinawa, Japan in 2000. The investigation involved three types

of prestressed concrete bridges and two types of FRP bridges. Overall, the authors concluded that FRP footbridges are more efficient when longer lifespan is needed in harshly corrosive locations.

## 2.4 Code Provisions

Predicting the unbonded tendon ultimate stress is presented in multiple codes such as ACI 318-18 ACI 440.4R-04, and AASHTO Load and Resistance Factor Design (2017). These codes do not provide equations for prestressing a hybrid application of bonded and unbonded tendons as there is a knowledge gap in understanding the behavior of hybrid applications.

ACI 318-18 calculates the approximate  $f_{ps}$  values at nominal flexural strength for unbonded tendons as shown in table 2.1.

**Table 2.1 Approximate values of  $f_{ps}$  at nominal flexural strength for unbonded tendons, (ACI 318-18)**

$\ell_n/h$	$f_{ps}$	
$\leq 35$	The least of:	$f_{se} + 10,000 + f'_c/(100\rho_p)$
		$f_{se} + 60,000$
		$f_{py}$
$> 35$	The least of:	$f_{se} + 10,000 + f'_c/(300\rho_p)$
		$f_{se} + 30,000$
		$f_{py}$

ACI 440.4R-04 calculates the unbonded tendon ultimate stress proposed by Naaman et al. (2002) shown in equations 2.2, 2.3, and 2.4. This method assumes compatibility of strains, as though the tendons were bonded, and uses a strain reduction factor  $\Omega$  to represent the tendons as unbonded.

$$f_p = f_{pe} + \Omega_u E_p \varepsilon_{cu} \left( \frac{d_p}{c_u} - 1 \right) \quad (2.2)$$

where,

$$\Omega_u = \frac{1.5}{L/d_p} \text{ (for one point loading)} \quad (2.3)$$

$$\Omega_u = \frac{3.0}{L/d_p} \text{ (for two point loading)} \quad (2.4)$$

AASHTO (2017) uses the following design equation to calculate the average stress in unbonded prestressing steel for rectangular or flanged sections.

$$f_{ps} = f_{se} + 900 \left( \frac{d_p - c}{l_e} \right) \leq f_{py} \quad (2.5)$$

where,

$$l_e = \left( \frac{2l_i}{2 + N_s} \right) \quad (2.6)$$

$l_i$  = length of the tendon between anchorages (in.)

$N_s$  = number of plastic hinges at supports assumed as:

- For simple spans.....0
- End spans of continuous units.....1
- Interior spans of continuous units.....2

## CHAPTER III

### 3. EXPERIMENTAL PROGRAM

#### 3.1 Introduction

The experimental program of this research is intended to determine the various effects of using CFRP/Steel tendons as unbonded elements with a bonded steel tendon. In hybrid prestressed beams, a bonded steel tendon is used to improve the ductility of the entire member and to overcome the brittle behavior of the CFRP tendon. This combination will benefit in utilizing smaller concrete sections and attaining longer span lengths.

Seven prestressed concrete T-beams were casted and tested in the Civil Engineering Laboratory at Rutgers University. All prestressed beams were simply supported using straight tendon profile and tested with four-point loading. In this experimental program, there were several parameters to be considered as listed below:

1. Area of the unbonded tendons,  $A_{ups}$
2. Unbonded tendons material (CFRP or Steel)
3. Depth of unbonded tendons

There will be four stages in the experimental process which are materials and preparation for casting beams, casting the beams, post-tensioning and testing the beams, and lastly data analysis. An outline of the tasks for the experimental process is shown below, which will be explained in more detail.

- A. Mechanical Testing
  - a. High Performance Concrete
  - b. Prestressing Steel
  - c. Steel Rebar
  - d. CFRP Tendons
- B. Casting Process
  - a. Installing the Tendon
  - b. Pre-tensioning Process
  - c. Casting the Concrete
- C. Testing
  - a. Post-tensioning Process
  - b. Installing Sensors
  - c. Testing Beam

## **3.2 Mechanical Properties Test**

### **3.2.1 High Performance Concrete**

The concrete mix design applied in the casting and testing of the beams are summarized in table 3.1. In order to create high performance concrete, silica fume and other materials were utilized in the mix. Strength testing was performed up to 28 days and is shown in table 3.2.

**Table 3.1 Mix Design Properties**

<b>Material</b>	<b>Weight</b>	<b>Volume</b>
Cement	224 lb	1.14 ft <sup>3</sup>
Silica Fume	22.4 lb	0.16 ft <sup>3</sup>
Rock (3/8")	341.39 lb	1.94 ft <sup>3</sup>
Sand	188.18 lb	1.15 ft <sup>3</sup>
Water	66.52 lb	1.07 ft <sup>3</sup>
HRWR	1225 mL	0.043 ft <sup>3</sup>

**Table 3.2 Concrete Mechanical Properties**

<b>Age</b>	<b>Compressive (psi)</b>	<b>Tensile (psi)</b>	<b>Modulus of Elasticity (ksi)</b>	<b>Cracking Strain (<math>\mu\epsilon</math>)</b>
1 day	9375	637	4259	150
3 days	9753	697	4372	159
7 days	10669	709	4630	153
14 days	12022	766	4993	153
28 days	13217	916	4911	186



### 3.2.2 Prestressing Steel

In this experimental program, grade 300 seven-wire stress relieved strands were used. The steel tendons had a diameter of 5/16 inches with an area of 0.058 in<sup>2</sup>. The yield strength, ultimate stress, and modulus of elasticity for the strands are 270, 300, and 32000 ksi.

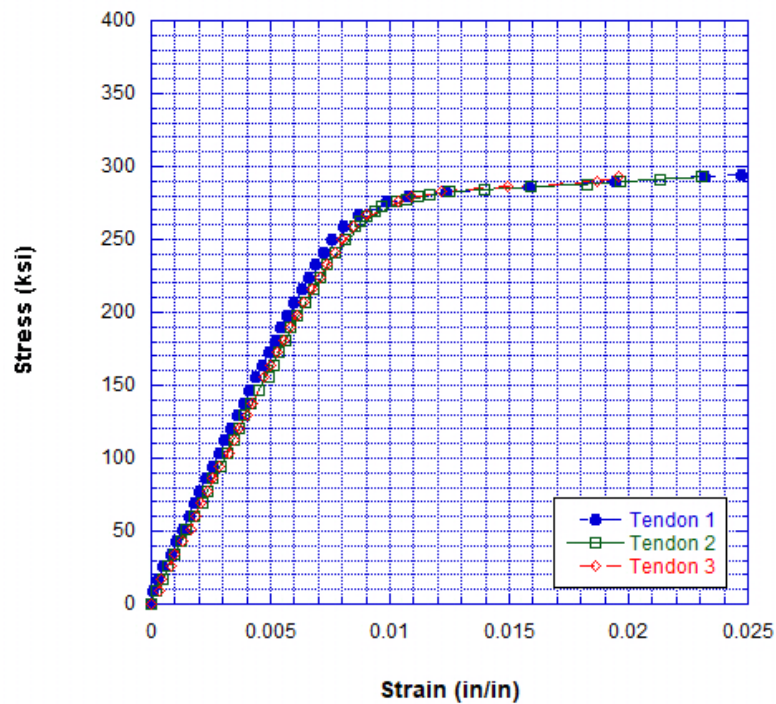


Figure 3.1 Tensile Testing of Steel Tendon

### 3.2.3 Steel Rebar

The flexural reinforcement provided in the prestressed concrete beams were built using #2 and #3 steel rebars. The rebars were tested in tension to determine the material properties as shown in figures 3.2 and 3.3. A summary of rebar properties are shown in table 3.3.

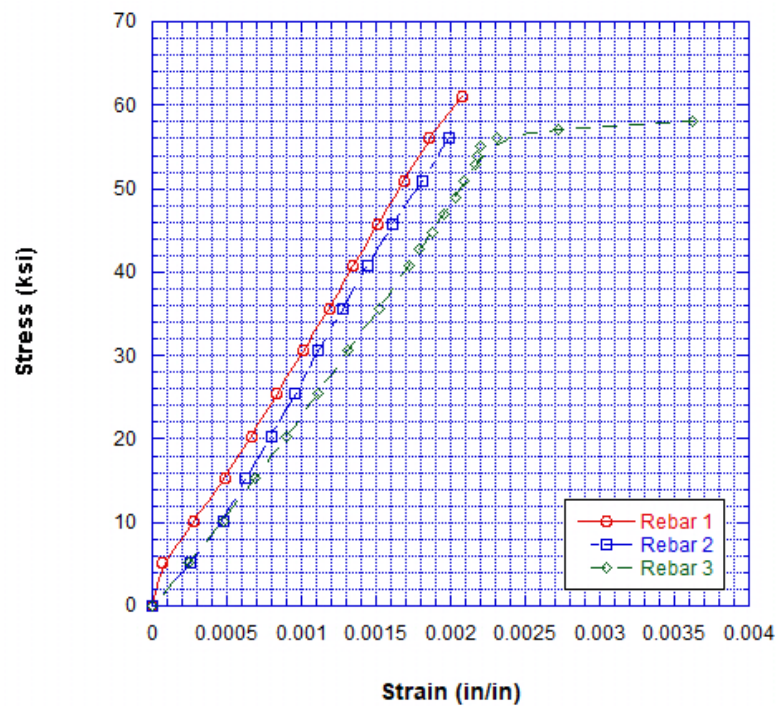


Figure 3.2 Tensile Testing of #2 Steel Rebar

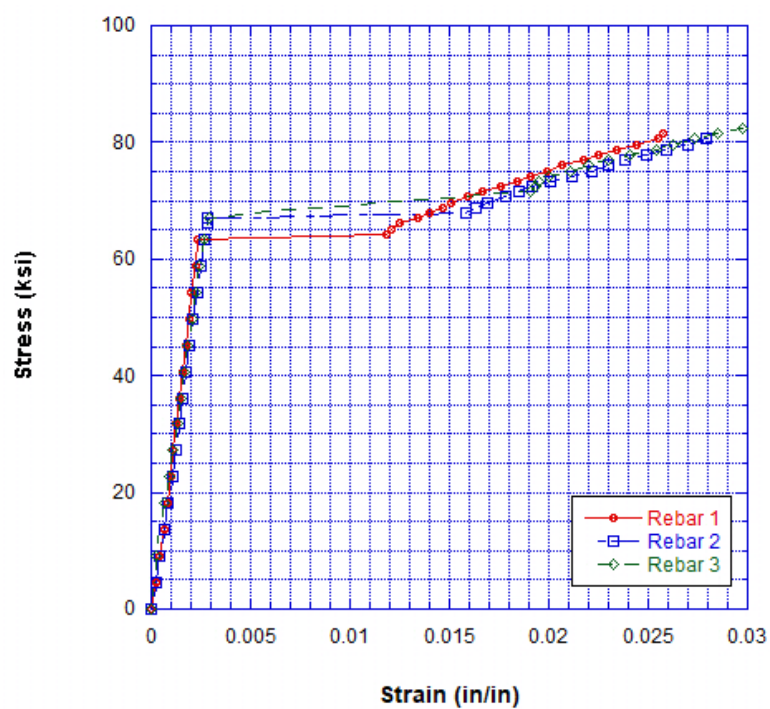


Figure 3.3 Tensile Testing of #3 Steel Rebar

**Table 3.3 Mechanical Properties of Steel Rebars**

<b>Diameter (in)</b>	<b>Area (in<sup>2</sup>)</b>	<b>Avg. <math>f_y</math> (ksi)</b>	<b>E (ksi)</b>
1/4	0.049	57	29,000
3/8	0.11	66	29,000

### 3.2.4 CFRP Tendons

Tokyo Rope CFRP tendons were utilized to post-tension the reinforced concrete beams. These beams were pre-tensioned with a steel tendon prior to post-tensioning with a CFRP tendon. The tendons were purchased from Tokyo Rope MFG. Company. These CFRP tendons have numerous benefits as compared to steel tendons. Tokyo Rope CFRP tendons are about 1/5 weight of steel tendons and are very flexible as they can be easily be winded into a coil. Also, the CFRP tendons have high resistance to corrosion and higher tensile strength when compared to steel tendons. The CFRP tendons used in this experimental program have a nominal area of 0.048 in<sup>2</sup> and 0.09 in<sup>2</sup>. The tendon with an area of 0.048 in<sup>2</sup> has an ultimate stress, ultimate strain, and modulus of elasticity of 355 ksi, 1.58% and 22480 ksi, respectively. The tendon with an area of 0.09 in<sup>2</sup> has an ultimate stress, ultimate strain, and modulus of elasticity of 354 ksi, 1.57% and 22480 ksi, respectively. These properties were provided by Tokyo Rope MFG. Company. The mechanical properties of the tendons are shown in table 3.4.

**Table 3.4 Mechanical Properties of CFRP Tendons (Tokyo Rope)**

<b>Diameter (in)</b>	<b>Area (in<sup>2</sup>)</b>	<b><math>f_{tu}</math> (ksi)</b>	<b>Ultimate Tensile Load (kips)</b>	<b><math>E_r</math> (psi 10<sup>6</sup>)</b>	<b>Ultimate Strain %</b>
0.295	0.048	355	17.09	22.48	1.58
0.413	0.09	354	31.70	22.48	1.57

### 3.3 Casting Process

Prior to casting the beams, steel cages and wooden molds for the beams were built. Also, strain gauges were installed at multiple locations on the flexural reinforcements and on the tendons as shown in figure 3.4. The casting process occurred in the Civil Engineering Laboratory at Rutgers University. An electric mixer with a volume of 9 cubic foot was used to mix and cast the beams. In order to perform mechanical properties testing, cylinders and prisms were casted alongside each beam.

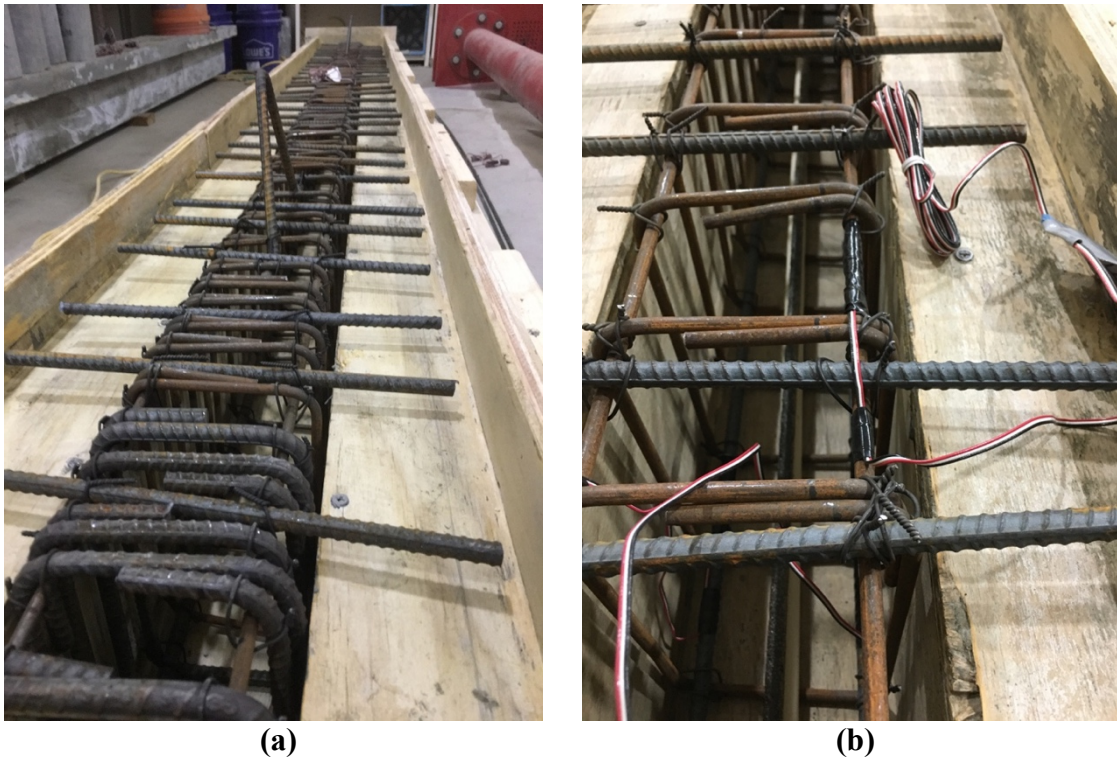


**Figure 3.4 Casting preparations (a) steel cage in the wooden mold, (b) strain gauges installed on multiple locations on the steel cage**

There were several stages that went into casting the beams shown below:

- Stage 1 involved installing the steel tendon and CPVC pipe through the wooden mold.
- Stage 2 involved pre-tensioning the steel tendon to a specified stress using anchors.
- Stage 3 involved the mixing and casting of the concrete as shown in figure 3.5.
- Stage 4 involved the post-tensioning of the CFRP tendons to a desired stress using specific anchors.





(a)

(b)

**Figure 3.5 Casting process (a) casting concrete in wooden mold, (b) concrete vibrated and leveled**

A typical cross-section and beam elevation of the beams tested are shown in figure 3.6. The dimensions of the beams are as follows:  $h = 10$  in,  $b = 12$  in,  $h_f = 2.25$  in, and  $b_w = 5$  in. The beam properties and parameters for all 7 beams are summarized in table 3.5.

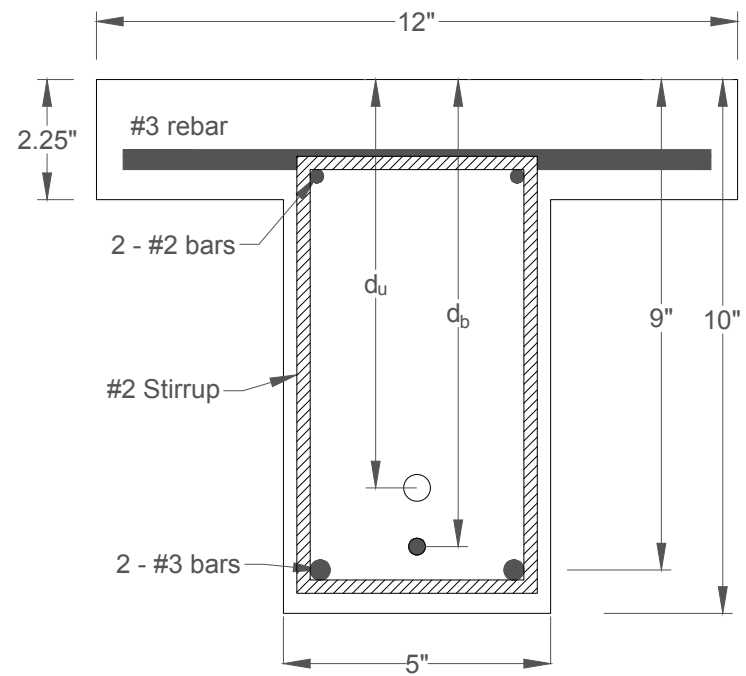
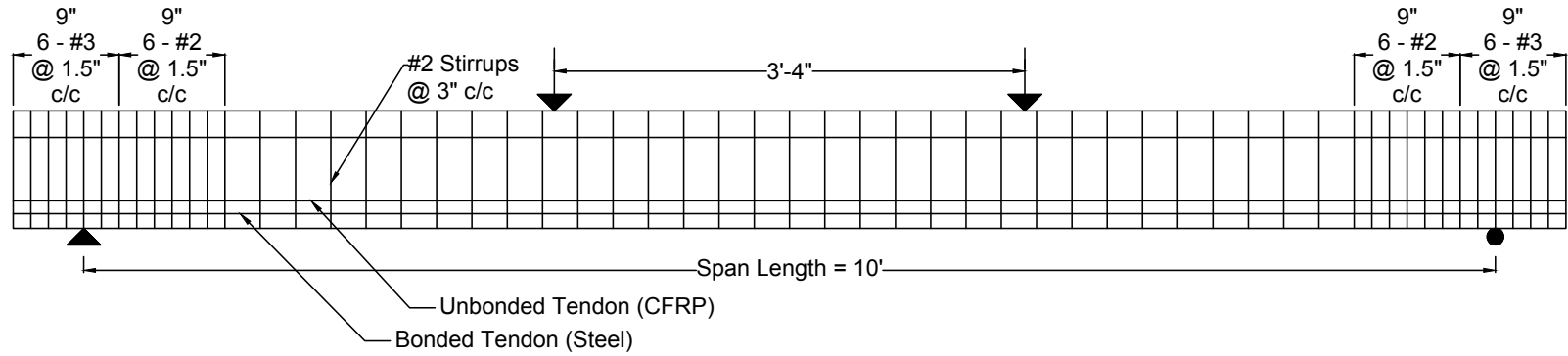


**Figure 3.6 Beam design and cross section details**

**Table 3.5 Summary of the beam properties and parameters**

Beam	Designation	$f'_c$ (ksi)	Bottom Tendon				Top Tendon				Length (in.)
			Material	Type	$A_{ps}$ (in <sup>2</sup> )	$d_b$ (in.)	Material	Type	$A_{ps}$ (in <sup>2</sup> )	$d_u$ (in.)	
B1	BS <sub>0.058</sub> D <sub>8.875</sub>	14.0	Steel	Bonded	0.058	8.875	-	-	-	-	120
B2	H-US <sub>0.058</sub> D <sub>6.65</sub>	11.3	Steel	Bonded	0.058	8.875	Steel	Unbonded	0.058	6.65	120
B3	H-UF <sub>0.048</sub> D <sub>6.65</sub>	14.0	Steel	Bonded	0.058	8.875	CFRP Tokyo	Unbonded	0.048	6.65	120
B4	H-UF <sub>0.09</sub> D <sub>6.65</sub>	12.4	Steel	Bonded	0.058	8.875	CFRP Tokyo	Unbonded	0.09	6.65	120
B5	H-UF <sub>0.048</sub> D <sub>7.65</sub>	13.9	Steel	Bonded	0.058	8.875	CFRP Tokyo	Unbonded	0.048	7.65	120
B6	H-UF <sub>0.09</sub> D <sub>7.65</sub>	14.5	Steel	Bonded	0.058	8.875	CFRP Tokyo	Unbonded	0.09	7.65	120
B7	BS-BS <sub>0.058</sub> D <sub>6.65</sub>	13.2	Steel	Bonded	0.058	8.875	Steel	Bonded	0.058	6.65	120

All beams tested have a bonded steel tendon with an area of 0.058 in<sup>2</sup> at a depth of 8.875 inches from the top of the beam. The letters in the beam designation column are described as below:

H - Hybrid

B - Bonded

U - Unbonded

F - CFRP tendon

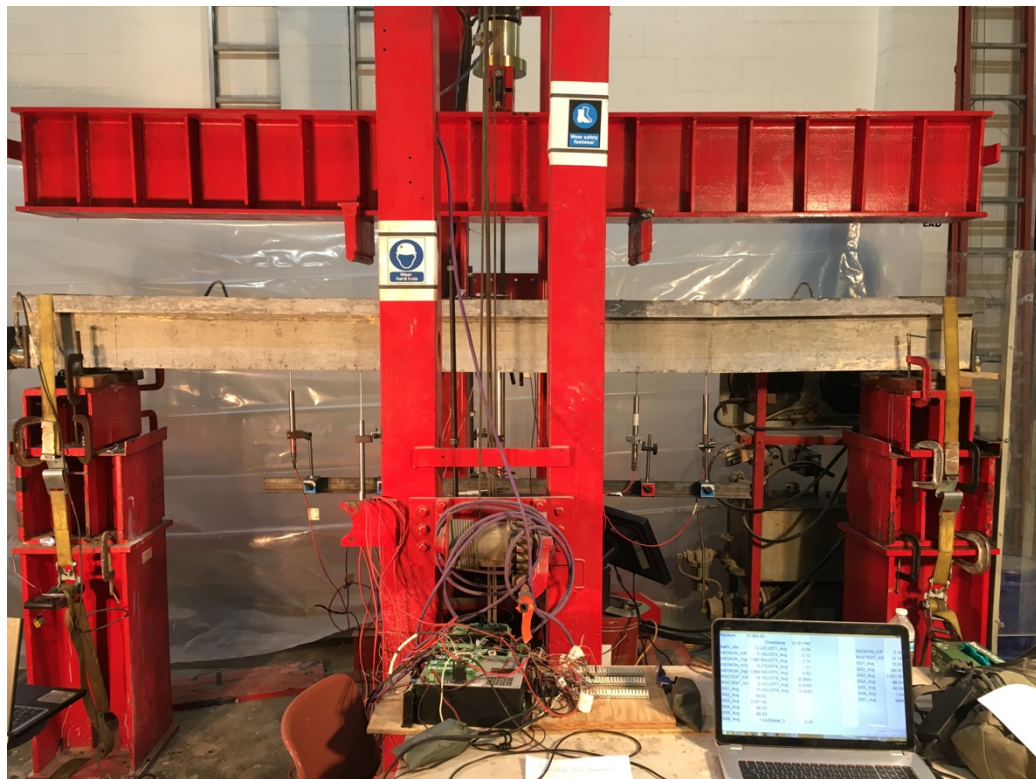
S - Steel tendon

D - Depth from top of beam



### 3.4 Testing Process

Testing the prestressed concrete beams occurred on or around the concrete age of 28 days. The day before testing, the beam was post-tensioned, placed on the testing machine, and sensors were installed. The compressive strength and the cracking strain of the concrete are about 13 ksi and 166  $\mu\epsilon$ , respectively around 28 days. Each beam has strain gauges, load cells, and linear variable differential transformers (LVDTs) installed at various locations on the beams. These sensors and equipment were used to measure the deflections, stresses, and strains of the concrete beams and the tendons. Figures 3.7 and 3.8 shows the testing setup and graphic representation of the locations of the strain gauges, load cells, and LVDTs on the beams tested. Also, the description and purpose of the sensors are summarized in table 3.6.





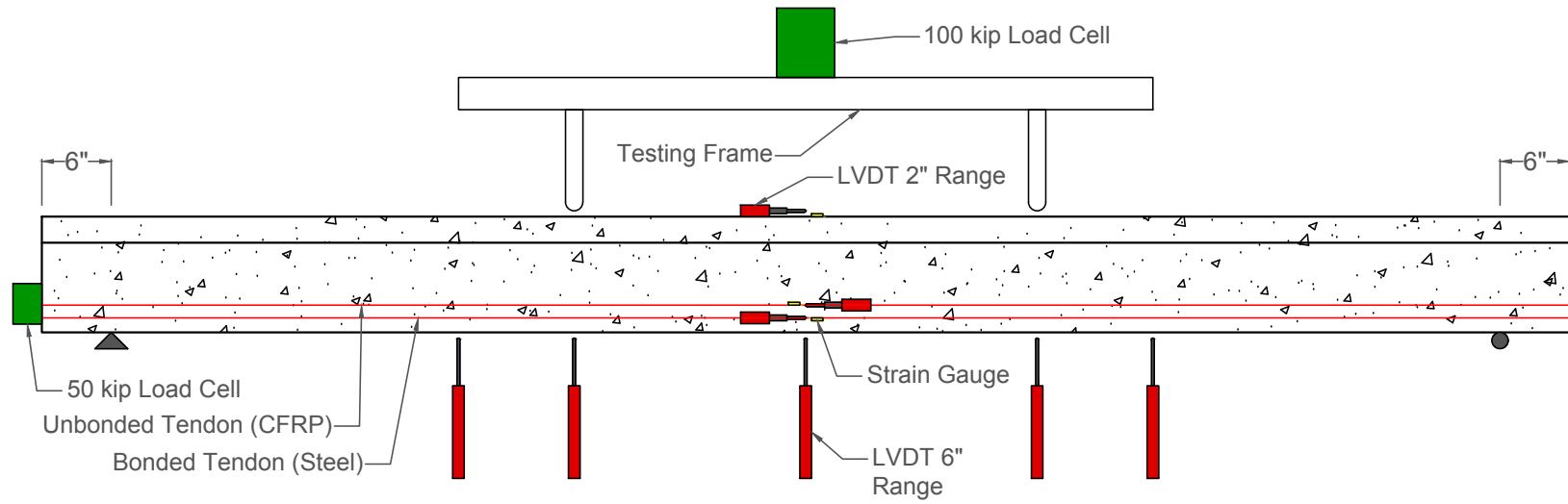


**Figure 3.7 Beam testing setup**



**Figure 3.8 Location of sensors used during beam testing**

Table 3.6 Overview and description of sensors used during testing

Sensors	Description
 <p><b>Linear Variable Differential Transformer (LVDT)</b></p>	<p>LVDTs were used to measure the deflections and strains of the beam at multiple locations. Two kinds of LVDTs were bought from RDP, which were the 6 inch and 2 inch range sensors.</p>
 <p><b>Load Cell – 100 kip</b></p>	<p>To monitor the load applied externally on the beam during testing, a 100 kip load cell was attached to the hydraulic actuator on top of the testing machine.</p>
 <p><b>Strain Gauge - Vishay</b></p>	<p>Strain gauges were installed on the top and bottom of the steel reinforcing stirrups, on top of the concrete beam, and on the prestressing tendons.</p>
 <p><b>Load Cell – 250 kN</b></p>	<p>To monitor the force in the prestressing tendons while jacking and testing, a 50 kip load cell was used.</p>

## CHAPTER IV

### 4. TEST RESULTS

#### 4.1 Introduction

Only seven beams were tested for the experimental process, however, as shown in the figures below, the beam H-US<sub>0.058</sub> D<sub>7.65</sub> was included for better analysis of the results. The results in this chapter includes deflection at mid-span, ultimate load capacity, stress and strain in steel reinforcement, tendons, and concrete, crack numbers, width and spacing for all beams. All results will be analyzed and discussed.

#### 4.2 Cracking Behavior

The cracking of concrete occurs when the stress reaches the modulus of rupture. This is where the tensile stress is shifted to the steel reinforcement. The steel rebars extend as the stress increases, and the cracks widen and propagate towards the top of the beams until failure occurs. The rate of stress in the prestressing tendons increases considerably after cracks occur. When the flexural steel reinforcement yields, the rate of stress in the tendons escalates further until beam failure.

During beam testing, a digital micro camera was used with a software on the computer to take pictures of the cracks on both sides of the beam, as shown in figure 4.1. At different loading stages during testing, pictures of the cracks were taken, and the crack widths were measured after testing. Also, the total number of cracks were recorded throughout each beam and the results are shown in table 4.1 The change in the unbonded

tendon area, depth, and material has a significant effect on the crack width throughout the beam.

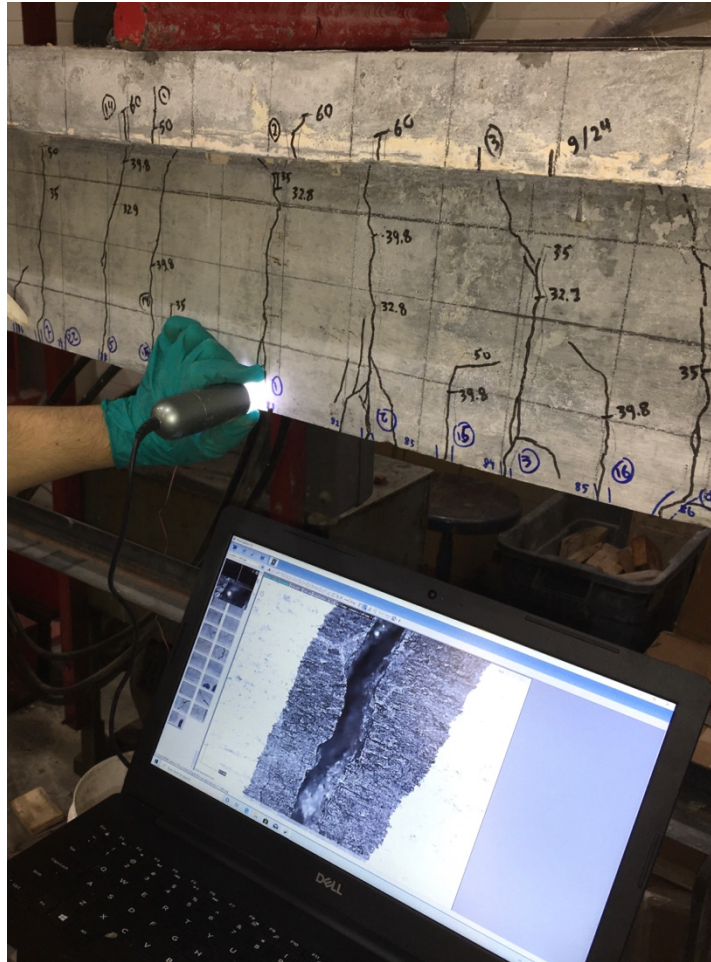


**Figure 4.1 Crack mapping during beam testing**

The cracking performance for the tested beams was analyzed at the cracks located about 5 to 6 inches to the right of the center of the beam. These cracks are outlined in blue and shown in figures 4.2 and 4.3. ACI 224R-01 specifies a maximum allowable crack width of 0.016 inches in reinforced concrete. Therefore, the applied load can be obtained and compared for all the cracks located at the same location for each beam with a crack width of 0.016 inches.

The effect of the unbonded tendon area at the same depth is shown in figure 4.4. When the area of the CFRP tendon increased for the unbonded tendon, there was an increase in the applied load to achieve the same crack width of 0.016 inches. Comparing beams H-UF<sub>0.048</sub>D<sub>6.65</sub> and H-UF<sub>0.09</sub>D<sub>6.65</sub>, there was a 38% increase in load to obtain the same crack width of 0.016 inches. As for beams H-UF<sub>0.048</sub>D<sub>7.65</sub> and H-UF<sub>0.09</sub>D<sub>7.65</sub>, there was a 15% increase in applied load. Considering the tendon material and the area shows that replacing an unbonded steel tendon with a CFRP tendon can achieve very similar results in terms of crack width. Beam H-UF<sub>0.048</sub>D<sub>6.65</sub> had an increase of 1.5% in load when compared to beam H-US<sub>0.058</sub>D<sub>6.65</sub>. When replacing the unbonded steel tendon with a bonded steel tendon, the beam was able to achieve a 16% increase in load to obtain the same crack width of 0.016. These results are summarized in table 4.2.

The effect of the unbonded tendons depth is also shown in figure 4.4. Comparing beams H-UF<sub>0.048</sub> D<sub>6.65</sub> and H-UF<sub>0.048</sub> D<sub>7.65</sub>, as well as H-UF<sub>0.09</sub> D<sub>6.65</sub> and H-UF<sub>0.09</sub> D<sub>7.65</sub>, there was an increase in load of 25% and 4.2%, respectively, to achieve the same maximum allowable crack width of 0.016 inches. Replacing the steel tendon with a CFRP tendon and increasing its depth, as shown with beams H-US<sub>0.058</sub> D<sub>6.65</sub> and H-UF<sub>0.048</sub>D<sub>7.65</sub>, there was an increase of 27% in load. These results are summarized in table 4.3.

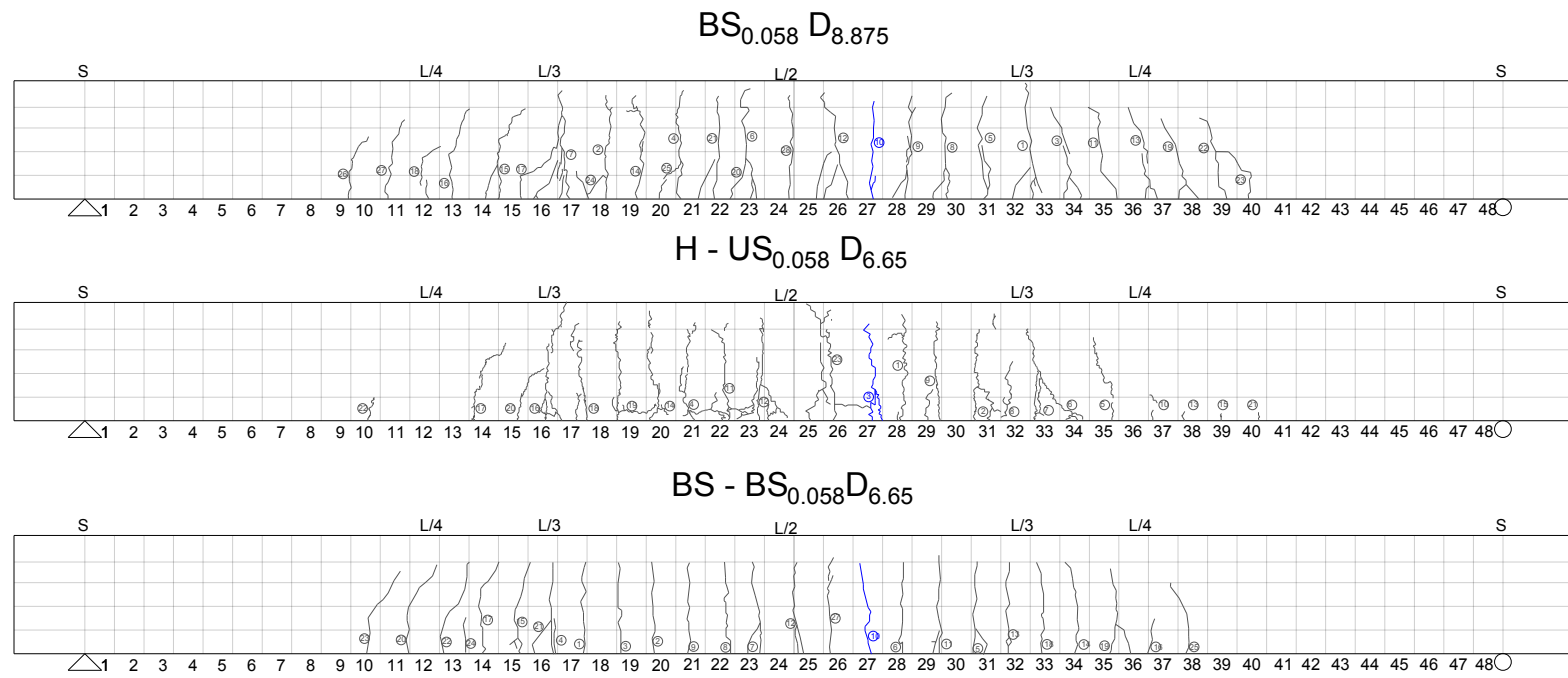


**Figure 4.2 Cracking Performance of Beams with Steel Tendons**

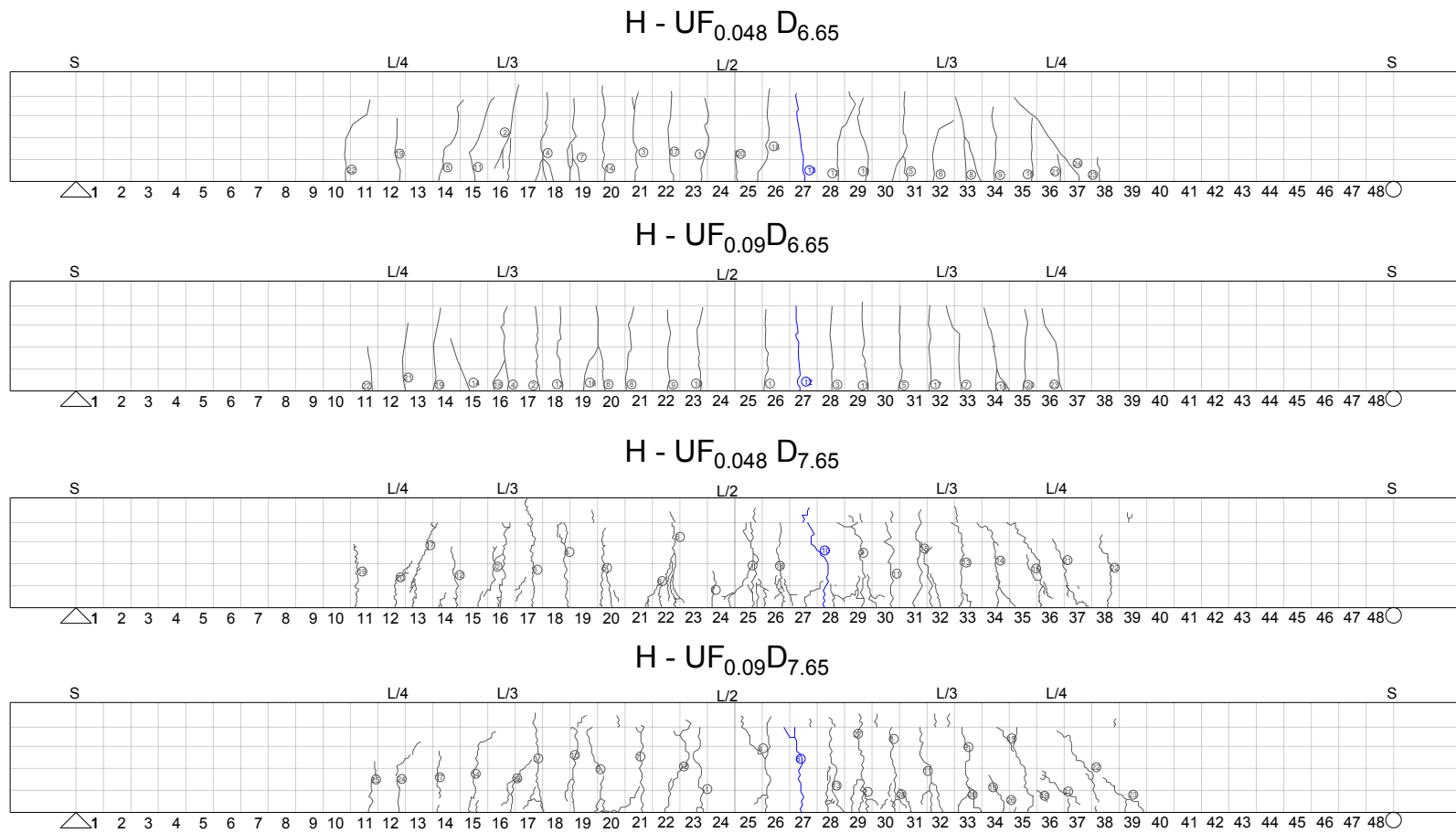


**Figure 4.3 Cracking Performance of Beams with CFRP Tendons**



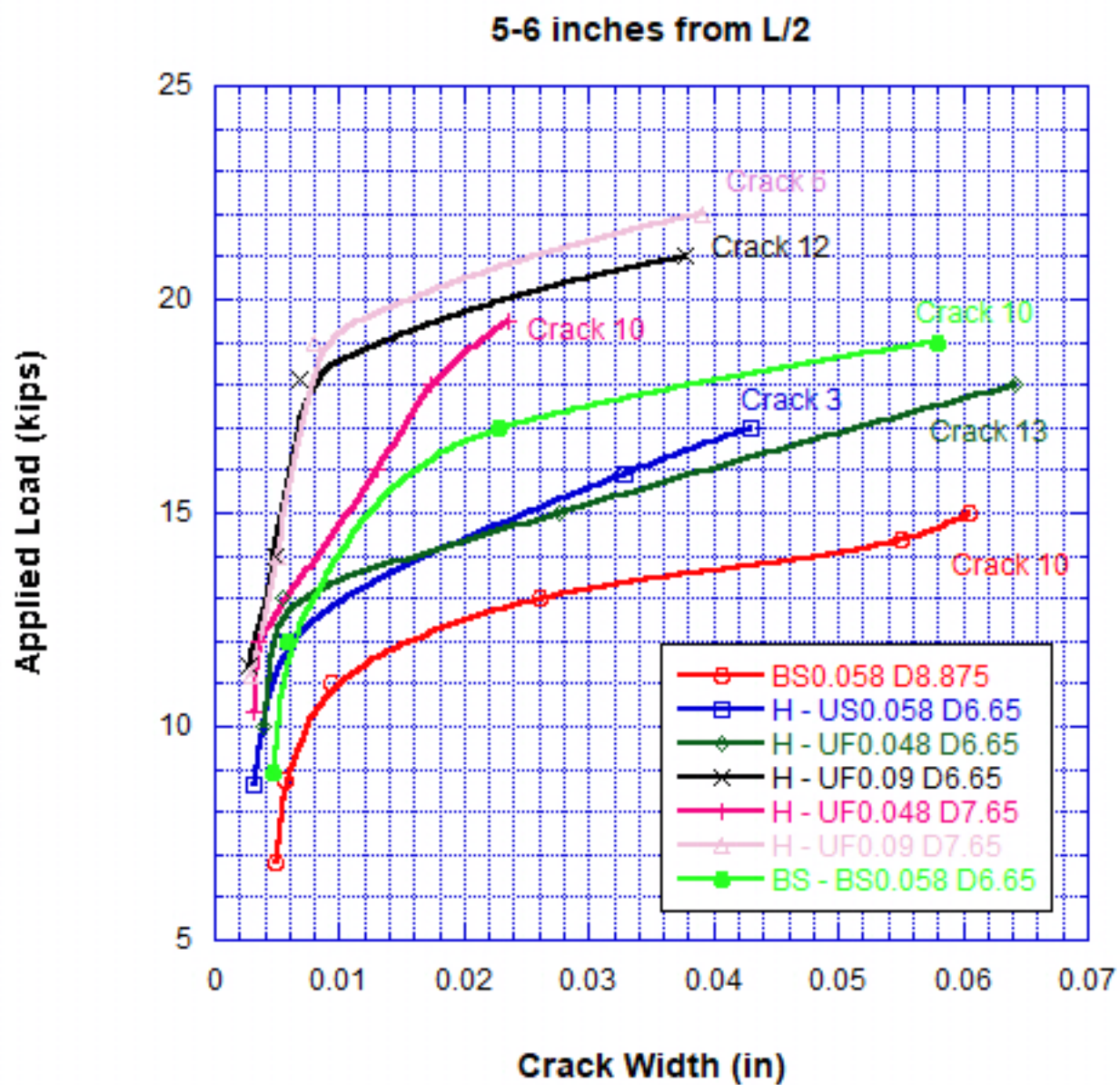


**Figure 4.4 Tendon Area, Depth, and Material Effect on Crack Width**

**Table 4.1 Summary of Crack Spacings, Number, and Widths**

	Beam Designation	Average Crack Spacing (in)	Number of Cracks	Maximum Crack Width (in)
1	BS <sub>0.058</sub> D <sub>8.875</sub>	2.80	28	0.0604
2	H-US <sub>0.058</sub> D <sub>6.65</sub>	3.00	23	0.0430
3	H-UF <sub>0.048</sub> D <sub>6.65</sub>	2.96	24	0.0642
4	H-UF <sub>0.09</sub> D <sub>6.65</sub>	2.89	23	0.0376
5	H-UF <sub>0.048</sub> D <sub>7.65</sub>	3.09	22	0.0236
6	H-UF <sub>0.09</sub> D <sub>7.65</sub>	3.09	28	0.0390
7	BS- BS <sub>0.058</sub> D <sub>6.65</sub>	3.00	25	0.0579

**Table 4.2 Tendon Area Effect on Applied Load at the same Crack Width Limit specified by ACI 224**

Beam Designation	Applied Load at 0.016 in. (kips)	% Difference
H-US <sub>0.058</sub> D <sub>6.65</sub>	13.8	CR
H-UF <sub>0.048</sub> D <sub>6.65</sub>	14.0	+1.5%
H-UF <sub>0.09</sub> D <sub>6.65</sub>	19.3	+40%
BS-BS <sub>0.058</sub> D <sub>6.65</sub>	16.0	+16%
H-UF <sub>0.048</sub> D <sub>6.65</sub>	14.0	CR
H-UF <sub>0.09</sub> D <sub>6.65</sub>	19.3	+38%
H-UF <sub>0.048</sub> D <sub>7.65</sub>	17.5	CR
H-UF <sub>0.09</sub> D <sub>7.65</sub>	20.1	+15%

**Table 4.3 Tendon Depth Effect on Applied Load at the same Crack Width**

Beam Designation	Applied Load at 0.016 in. (kips)	% Difference
H-US <sub>0.058</sub> D <sub>6.65</sub>	13.8	CR
H-UF <sub>0.048</sub> D <sub>6.65</sub>	14.0	+1.5%
H-UF <sub>0.048</sub> D <sub>7.65</sub>	17.5	+27%
H-UF <sub>0.048</sub> D <sub>6.65</sub>	14.0	CR
H-UF <sub>0.048</sub> D <sub>7.65</sub>	17.5	+25%
H-UF <sub>0.09</sub> D <sub>6.65</sub>	19.3	CR
H-UF <sub>0.09</sub> D <sub>7.65</sub>	20.1	+4.2%

### 4.3 Load – Deformation Behavior

To evaluate the performance of the prestressed concrete beams as the applied load increased, data was collected using the sensors discussed in chapter III. The measurements obtained from the data are directly related to the deformations which include load-deflection relationship, and load-strain relationship. These results will be discussed in detail.

#### 4.3.1 Load – Deflection Relationship

During the testing of the beams, the deflections were recorded at multiple locations along the beam. Table 4.4 shows a summary of the applied loads and measured mid-span deflections at several limit states. It is important to note that the ultimate load used was 80 – 90% of beam failure to prevent any discrepancies in crack widths at ultimate. For each beam, the deflection at mid-span is recorded at the cracking of concrete, yielding of the flexural reinforcing steel, yielding of the unbonded tendons, yielding of the bonded tendons, and on top of the concrete beam. The load-deflection graphs shown in Figures 4.5 – 4.8 are displayed in groups that illustrates the effects of the  $A_{ps}$  (unbonded), the depth of the unbonded tendons, and the unbonded tendon materials on the load-deflection performance. All beams tested had a bonded steel tendon with an area of 0.058 in<sup>2</sup> located at 8.875 inches from the top of the beam.

The first comparison was produced displaying the effect of the addition of a second tendon prestressed on top of the bonded pre-tensioned tendon. This additional tendon was either bonded or unbonded, creating a fully bonded beam or a hybrid beam, respectively. The tendon materials used for the unbonded beams were steel and CFRP. For BS<sub>0.058D8.875</sub> with only one bonded tendon, the capacity achieved was 13 kips with a

deflection of 1.18 inches. For H-US<sub>0.058</sub>D<sub>6.65</sub>, the capacity increased 23.08% to 16 kips with a 3.39% reduction in deflection to 1.14 inches when compared to BS<sub>0.058</sub>D<sub>8.875</sub>. When changing the unbonded tendon material to CFRP for H-UF<sub>0.048</sub>D<sub>6.65</sub>, the capacity increased 15.38% to 15 kips with a 0.85% reduction in deflection to 1.17 inches when compared to BS<sub>0.058</sub>D<sub>8.875</sub>. When using a second bonded tendon creating a fully bonded beam for BS-BS<sub>0.058</sub> D<sub>6.65</sub>, the capacity increased 30.77% to 17 kips with an 11.02% reduction in deflection to 1.05 inches when compared to BS<sub>0.058</sub>D<sub>8.875</sub>. When comparing a hybrid steel bonded with steel unbonded beam (H-US<sub>0.058</sub>D<sub>6.65</sub>) to a fully bonded beam (BS-BS<sub>0.058</sub> D<sub>6.65</sub>), the fully bonded beam achieved a 6.25% increase in capacity and a 7.89% reduction in deflection.

The area of the unbonded tendons while positioned at the same depth was also investigated. Comparing beams H-US<sub>0.058</sub>D<sub>6.65</sub> and H-UF<sub>0.048</sub>D<sub>6.65</sub>, the results show that when post-tensioning CFRP tendons as compared to steel tendons with similar diameters, there was a slightly lower ultimate load capacity and higher deflection. For H-US<sub>0.058</sub>D<sub>6.65</sub> the capacity achieved was 16 kips with a deflection of 1.14 inches. For H-UF<sub>0.048</sub>D<sub>6.65</sub> the capacity achieved was 15 kips with a deflection of 1.17 inches, which has 6.25% reduction in capacity and 2.63% increase in deflection compared to H-US<sub>0.058</sub>D<sub>6.65</sub>. The area of the CFRP tendon is slightly smaller than the steel tendon. If the area of the CFRP tendon was the same as the steel tendon, then it's possible that using the CFRP tendon could achieve the same or higher capacity with a lower deflection. A larger area CFRP tendon was post-tensioned at the same depth in H-UF<sub>0.09</sub>D<sub>6.65</sub> and this resulted in achieving a 12.5% increase in capacity to 18 kips and a 29% reduction in deflection to 0.81 inches than the use of the steel tendon in H-US<sub>0.058</sub>D<sub>6.65</sub>. Comparing beams with an

unbonded tendon depth of 7.65 inches from the top of the beam, the results show that H-US<sub>0.058</sub>D<sub>7.65</sub> achieved a capacity of 17 kips with a deflection of 0.87 inches. For H-UF<sub>0.048</sub>D<sub>7.65</sub>, the capacity increased 5.88% to 18 kips and the deflection increased 85.06% to 1.61 inches when compared to H-US<sub>0.058</sub>D<sub>7.65</sub>. For H-UF<sub>0.09</sub>D<sub>7.65</sub>, the capacity increased 29.41% to 22 kips and the deflection increased 129.89% to 2 inches when compared to H-US<sub>0.058</sub>D<sub>7.65</sub>.

The depth of the unbonded tendons while maintaining the same tendon area was also examined in the hybrid beams. Comparing beams H-US<sub>0.058</sub>D<sub>6.65</sub> to H-UF<sub>0.048</sub>D<sub>7.65</sub> and H-US<sub>0.058</sub>D<sub>7.65</sub>, the results show that when post-tensioning a steel tendon with the same area at a lower depth, the ultimate load capacity increased and the ultimate deflection decreased. However, when post-tensioning the CFRP tendon with similar area at a lower depth, the ultimate load capacity and deflection both increased. For H-US<sub>0.058</sub>D<sub>6.65</sub> the capacity achieved was 16 kips with a deflection of 1.14 inches. For H-UF<sub>0.048</sub>D<sub>7.65</sub> the capacity achieved was 18 kips with a deflection of 1.61 inches which has 12.5% increase in capacity and 41.22% increase in deflection compared to H-US<sub>0.058</sub>D<sub>6.65</sub>. For H-US<sub>0.058</sub>D<sub>7.65</sub> the capacity achieved was 17 kips with a deflection of 0.87 inches which has 6.25% increase in capacity and 23.68% decrease in deflection compared to H-US<sub>0.058</sub>D<sub>6.65</sub>. Comparing beams H-UF<sub>0.048</sub>D<sub>6.65</sub> to H-UF<sub>0.048</sub>D<sub>7.65</sub>, the results show that when post-tensioning a CFRP tendon with the same area at a lower depth, the ultimate load capacity increased as well as the ultimate deflection. The same results were observed for beams H-UF<sub>0.09</sub>D<sub>6.65</sub> to H-UF<sub>0.09</sub>D<sub>7.65</sub>. For H-UF<sub>0.048</sub>D<sub>7.65</sub> the capacity achieved was 18 kips with a deflection of 1.61 inches which has 20% increase in capacity and 37.61% increase in deflection compared to H-UF<sub>0.048</sub>D<sub>6.65</sub>. For H-UF<sub>0.09</sub>D<sub>7.65</sub> the capacity

achieved was 22 kips with a deflection of 2 inches which has 22.22% increase in capacity and 146.91% increase in deflection compared to H-UF<sub>0.09</sub>D<sub>6.65</sub>.

**Table 4.4 Summary of applied loads and measured mid-span deflections at various limit states**

Beam Designation	P <sub>cr</sub> (kip)	Δ <sub>cr</sub> (in)	P <sub>y</sub> (kip)	Δ <sub>y</sub> (in)	P <sub>py (B)</sub> (kip)	Δ <sub>py (B)</sub> (in)	P <sub>py (U)</sub> (kip)	Δ <sub>py (U)</sub> (in)	80-90% P <sub>u</sub> (kip)	80-90% Δ <sub>u</sub> (in)	P <sub>u</sub> (kip)	Δ <sub>u</sub> (in)
BS <sub>0.058</sub> D <sub>8.875</sub>	5.70	0.05	-	-	11.13	0.58	-	-	13	1.18	15.10	1.46
H-US <sub>0.058</sub> D <sub>6.65</sub>	7.38	0.10	15.85	1.07	-	-	17.69	2.35	16	1.14	17.71	2.36
H-UF <sub>0.048</sub> D <sub>6.65</sub>	6.45	0.11	13.10	0.59	14.80	1.05	-	-	15	1.17	18.46	3.58
H-UF <sub>0.09</sub> D <sub>6.65</sub>	8.39	0.09	-	-	17.49	0.71	-	-	18	0.81	22.49	2.88
H-UF <sub>0.048</sub> D <sub>7.65</sub>	8.42	0.14	15.39	0.68	-	-	-	-	18	1.61	19.77	2.58
H-UF <sub>0.09</sub> D <sub>7.65</sub>	9.11	0.13	15.75	0.48	-	-	-	-	22	2.00	24.09	2.96
BS-BS <sub>0.058</sub> D <sub>6.65</sub>	7.91	0.11	13.01	0.41	15.06	0.60	16.51	0.89	17	1.05	19.87	3.43
H-US <sub>0.058</sub> D <sub>7.65</sub>	8.72	0.10	14.73	0.44	16.87	0.82	-	-	17	0.87	19.37	2.11

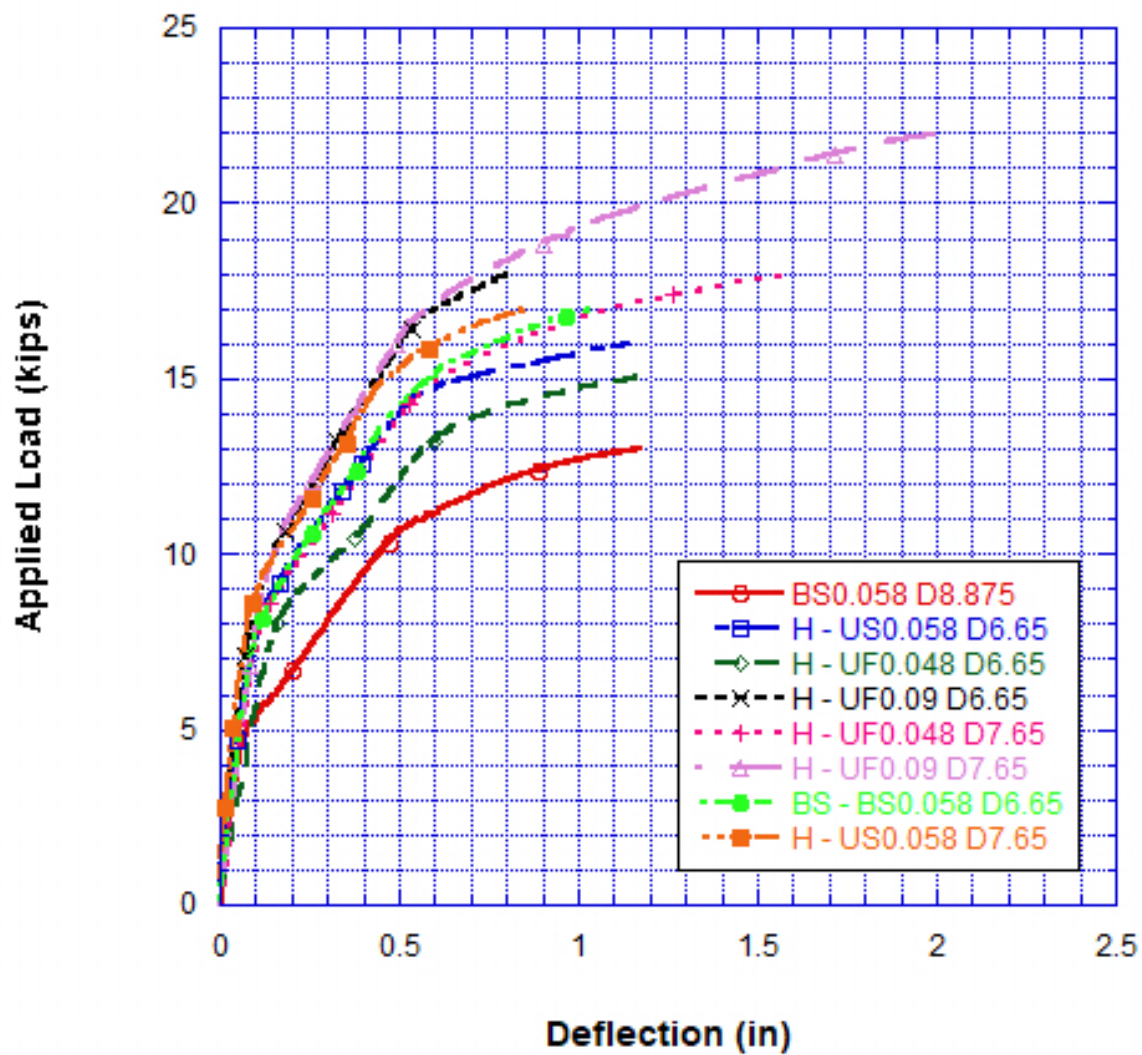


Figure 4.5 Load-deflection behavior of all prestressed concrete beams tested



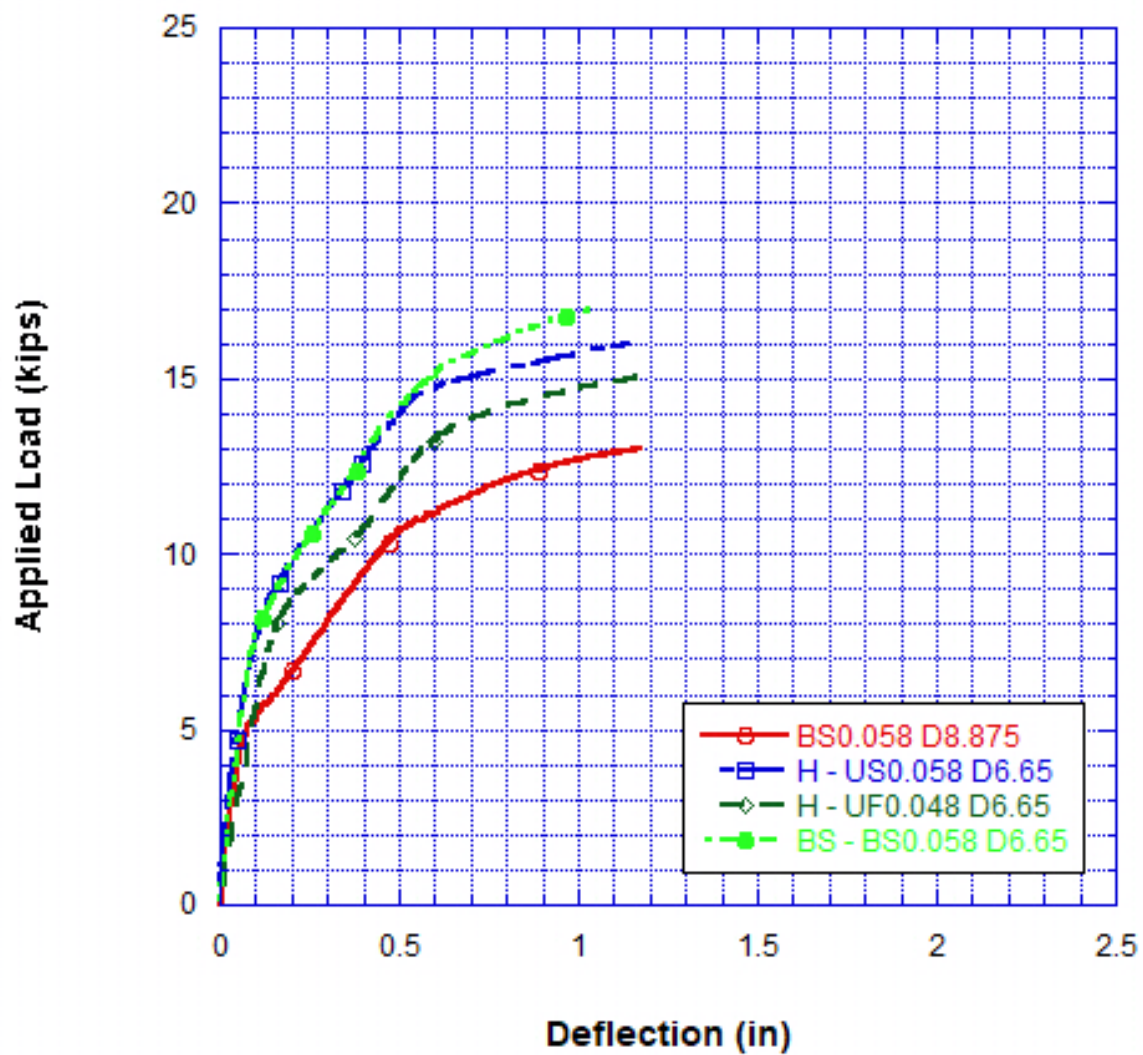


Figure 4.6 Effect of the hybrid combination compared to fully bonded steel tendons on the load-deflection behavior

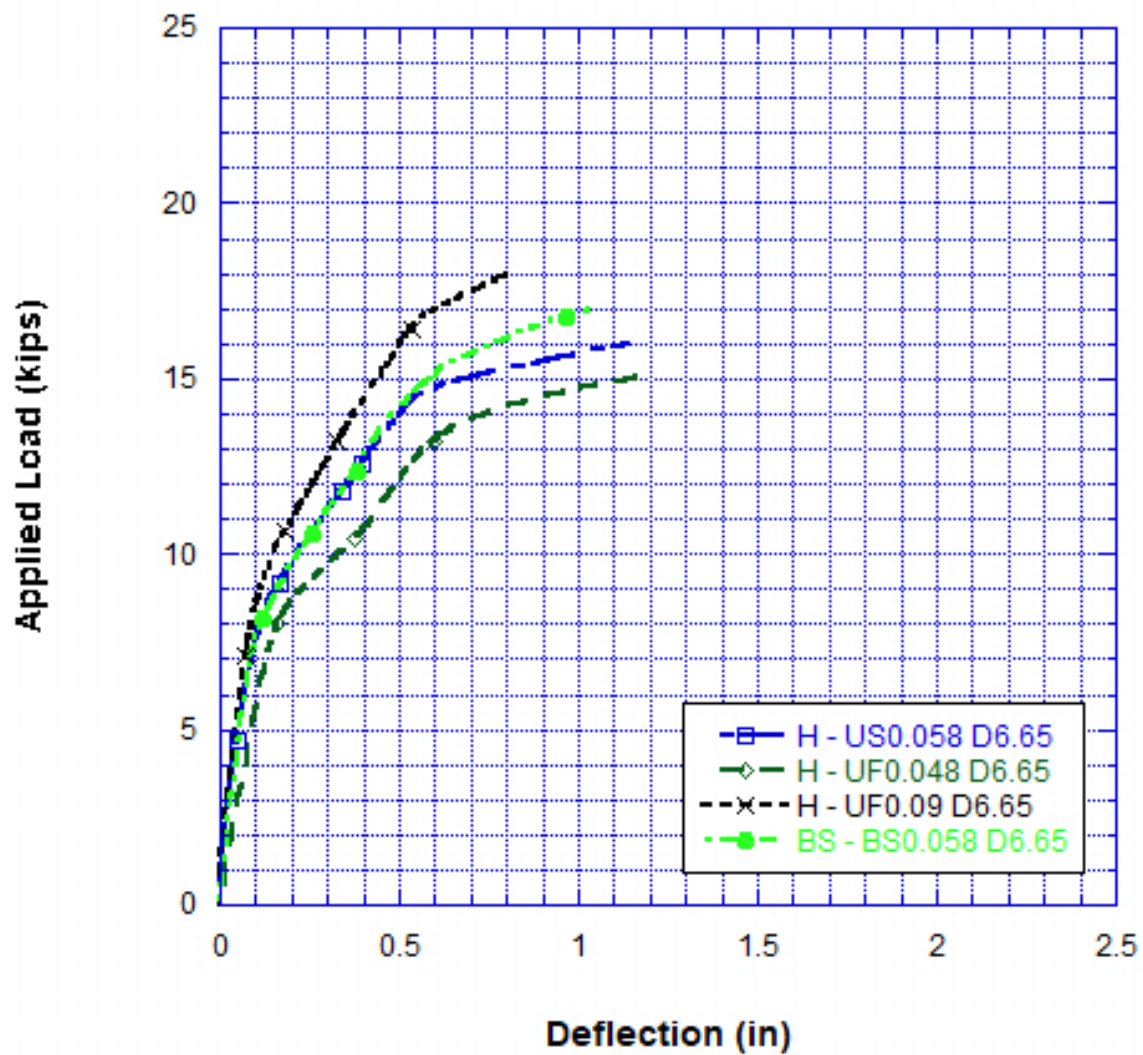


Figure 4.7 Effect of the area of the unbonded tendons on the load-deflection behavior at the same depth

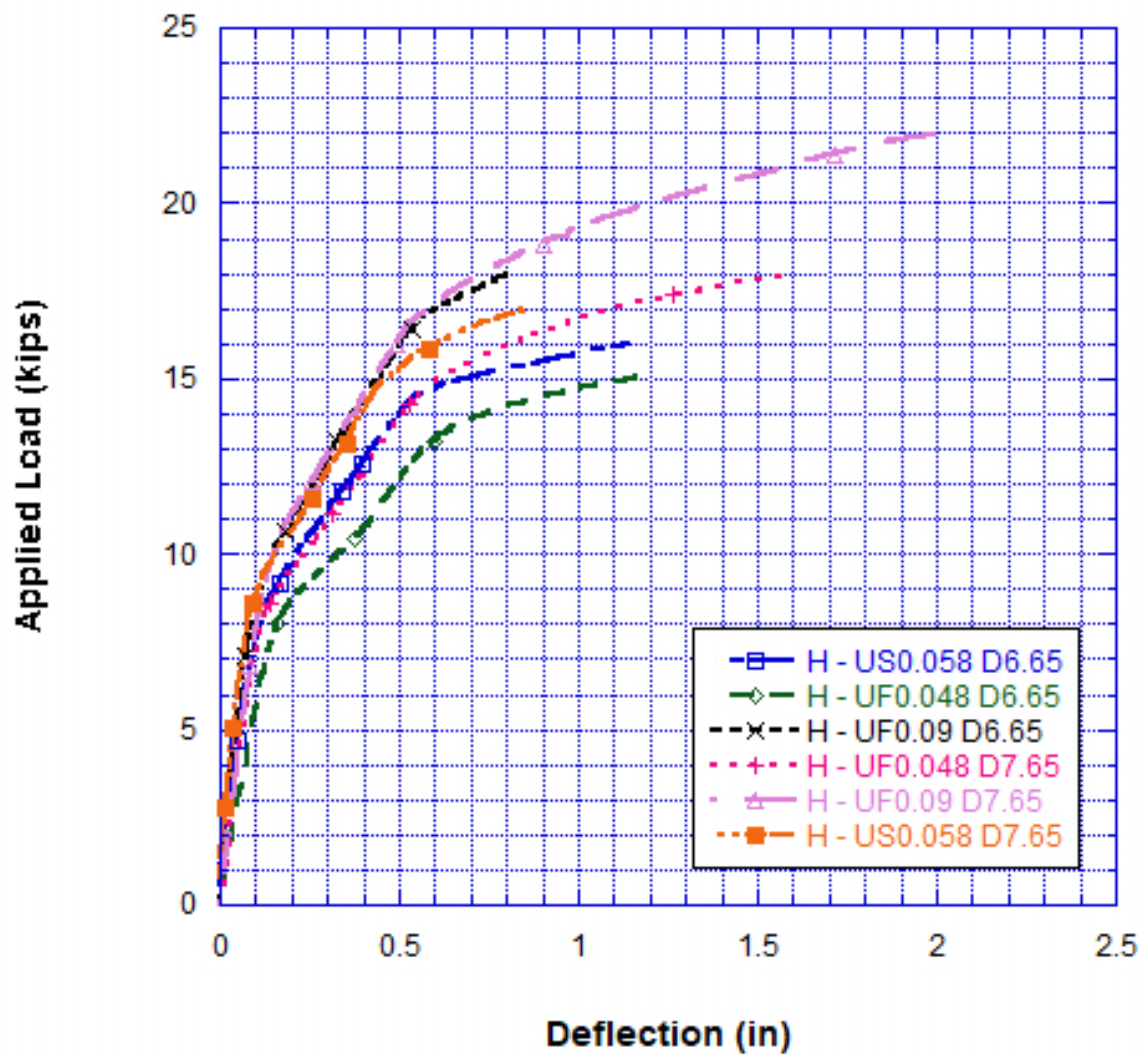


Figure 4.8 Effect of the unbonded tendons depth on the load-deflection behavior

### 4.3.2 Load – Strain Relationship

Strain measurements were recorded for all beams until failure at the flexural reinforcing steel, prestressing bonded and unbonded tendons, and at the top concrete fibers. As shown in figure 4.9, LVDT's and strain gauges were used to measure the strain at the maximum moment section and at other locations of the beam. These measured values are essentially recorded to understand the change in strain while testing to show the depth of the neutral axis at different periods of loading. Table 4.5 summarizes the ultimate strain at the extreme concrete fibers obtained from strain gauges. In the graphs showing the bottom rebar tensile strain for beams BS<sub>0.058</sub> D<sub>8.875</sub> and H - UF<sub>0.09</sub> D<sub>6.65</sub>, the strain gages stopped reading during the testing. For the bonded tendon strain in beam H – UF<sub>0.048</sub> D<sub>7.65</sub>, the strain gage stopping reading during the testing as well.



**Figure 4.9 Hybrid beam showing LVDT's at mid-span profile for strain profile measurement**

**Table 4.5 Measured compressive strain in concrete at extreme top fiber at failure load**

	Beam Designation	$\epsilon_{cu}$
1	BS <sub>0.058</sub> D <sub>8.875</sub>	-
2	H - US <sub>0.058</sub> D <sub>6.65</sub>	0.0022
3	H - UF <sub>0.048</sub> D <sub>6.65</sub>	0.0032
4	H - UF <sub>0.09</sub> D <sub>6.65</sub>	0.0057
5	H - UF <sub>0.048</sub> D <sub>7.65</sub>	0.0026
6	H - UF <sub>0.09</sub> D <sub>7.65</sub>	0.0024
7	BS-BS <sub>0.058</sub> D <sub>6.65</sub>	0.003
8	H - US <sub>0.058</sub> D <sub>7.65</sub>	0.0029



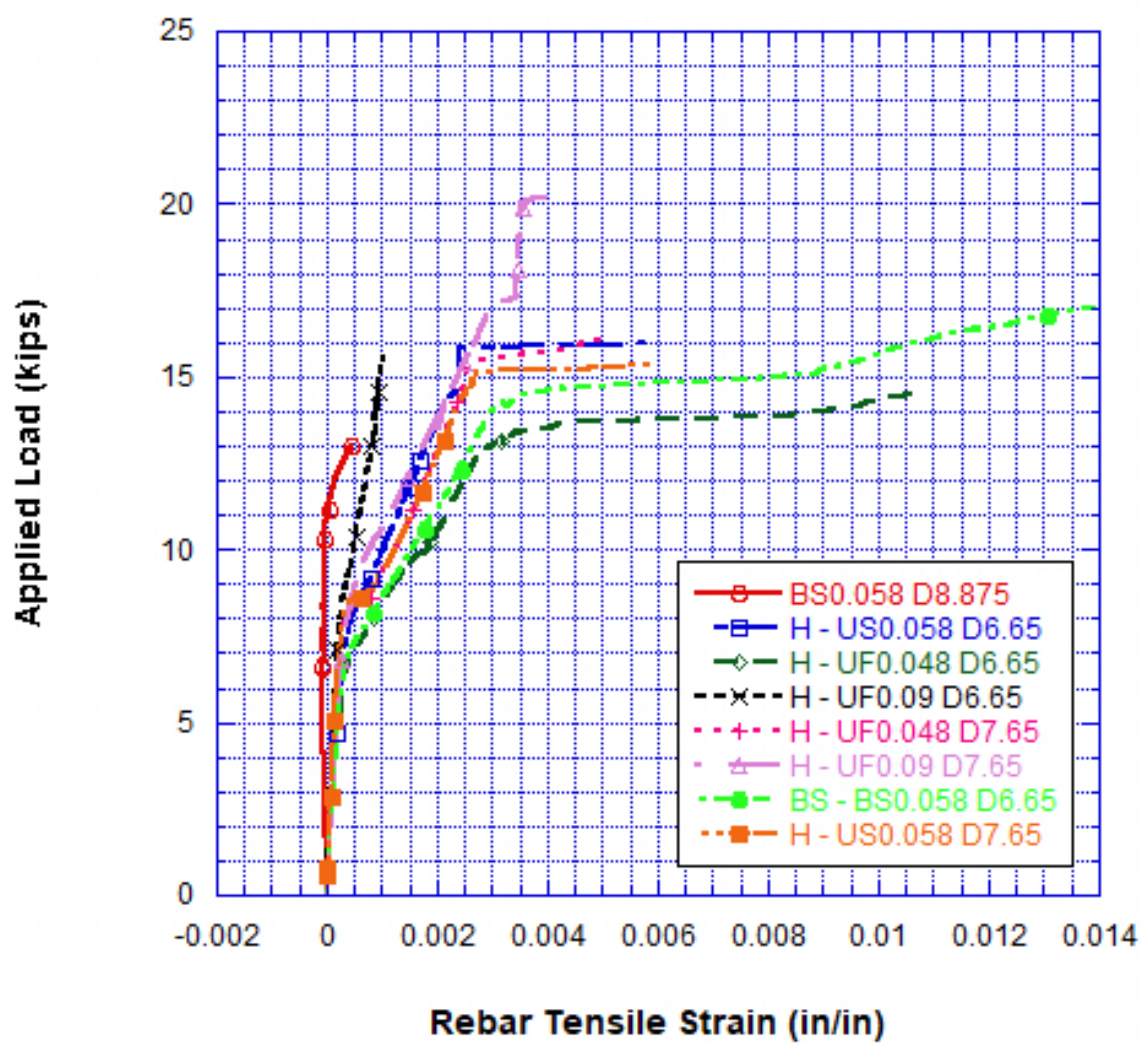


Figure 4.10 Load-strain behavior of the steel rebar strain for all prestressed concrete beams tested

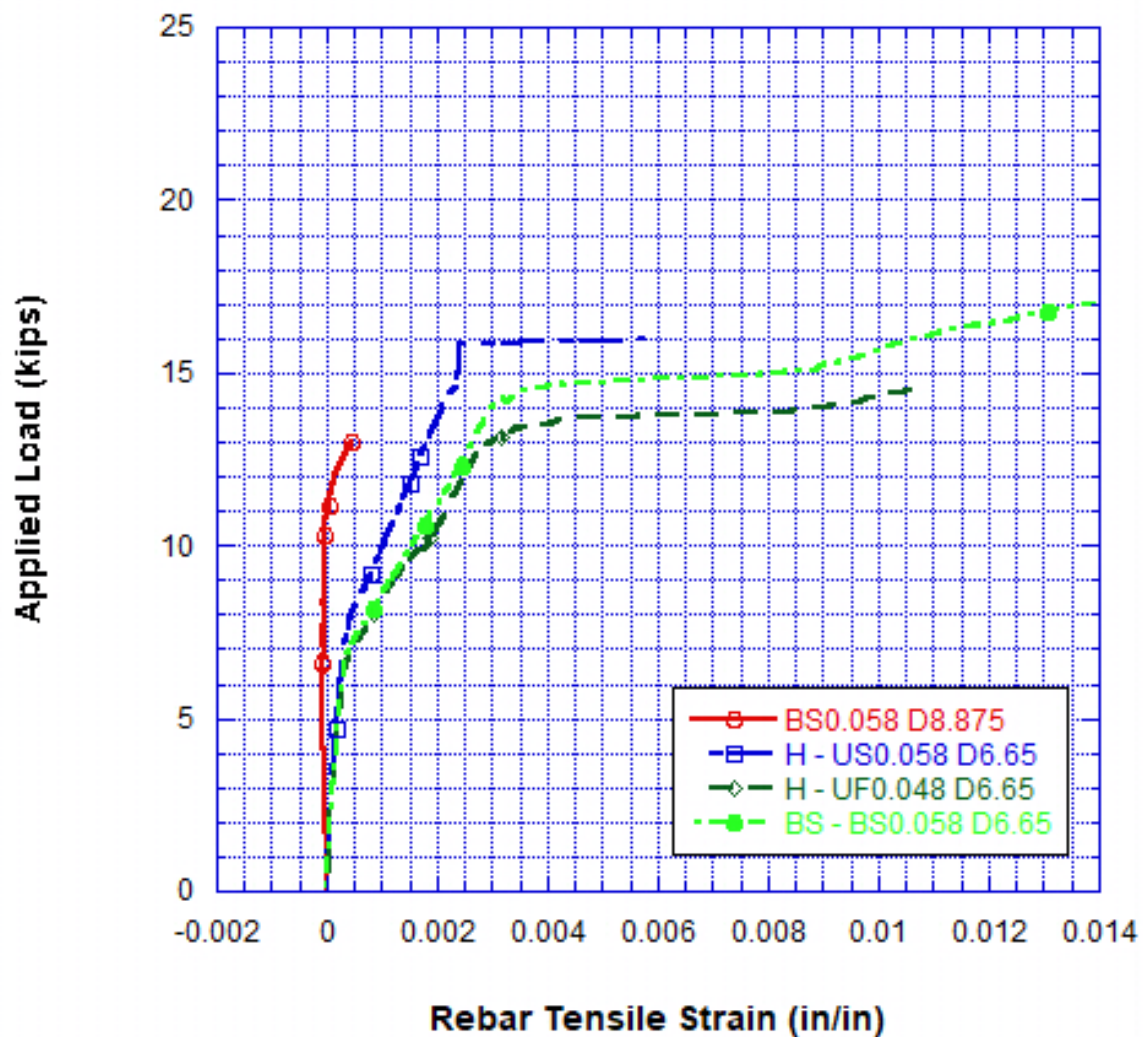


Figure 4.11 Load-strain behavior of the steel rebar strain for the hybrid combination compared to fully bonded steel tendons

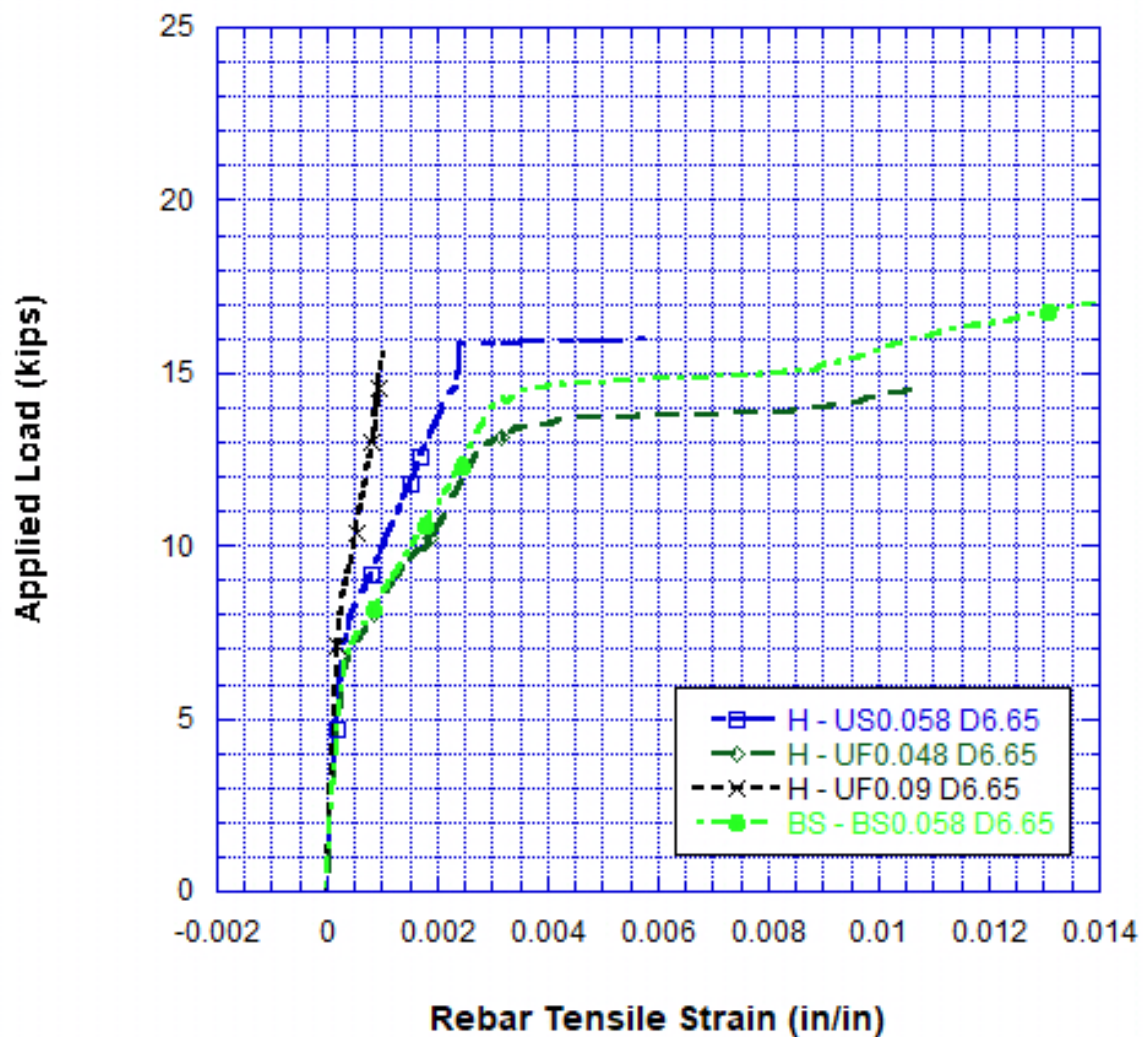


Figure 4.12 Effect of the area of the unbonded tendons at the same depth on the load-strain behavior of the steel rebar strain



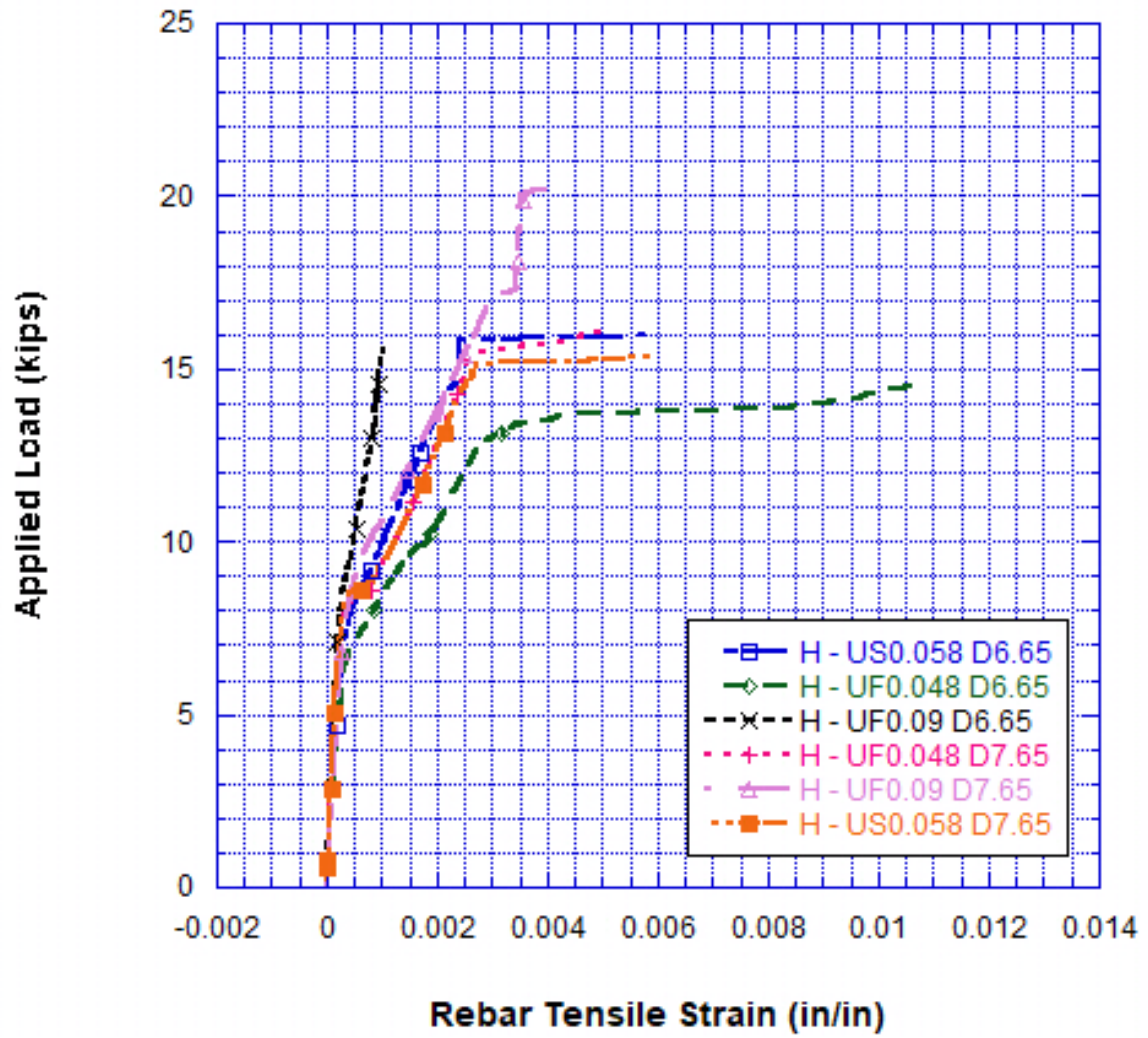


Figure 4.13 Effect of the unbonded tendons depth on the load-strain behavior of the steel rebar strain

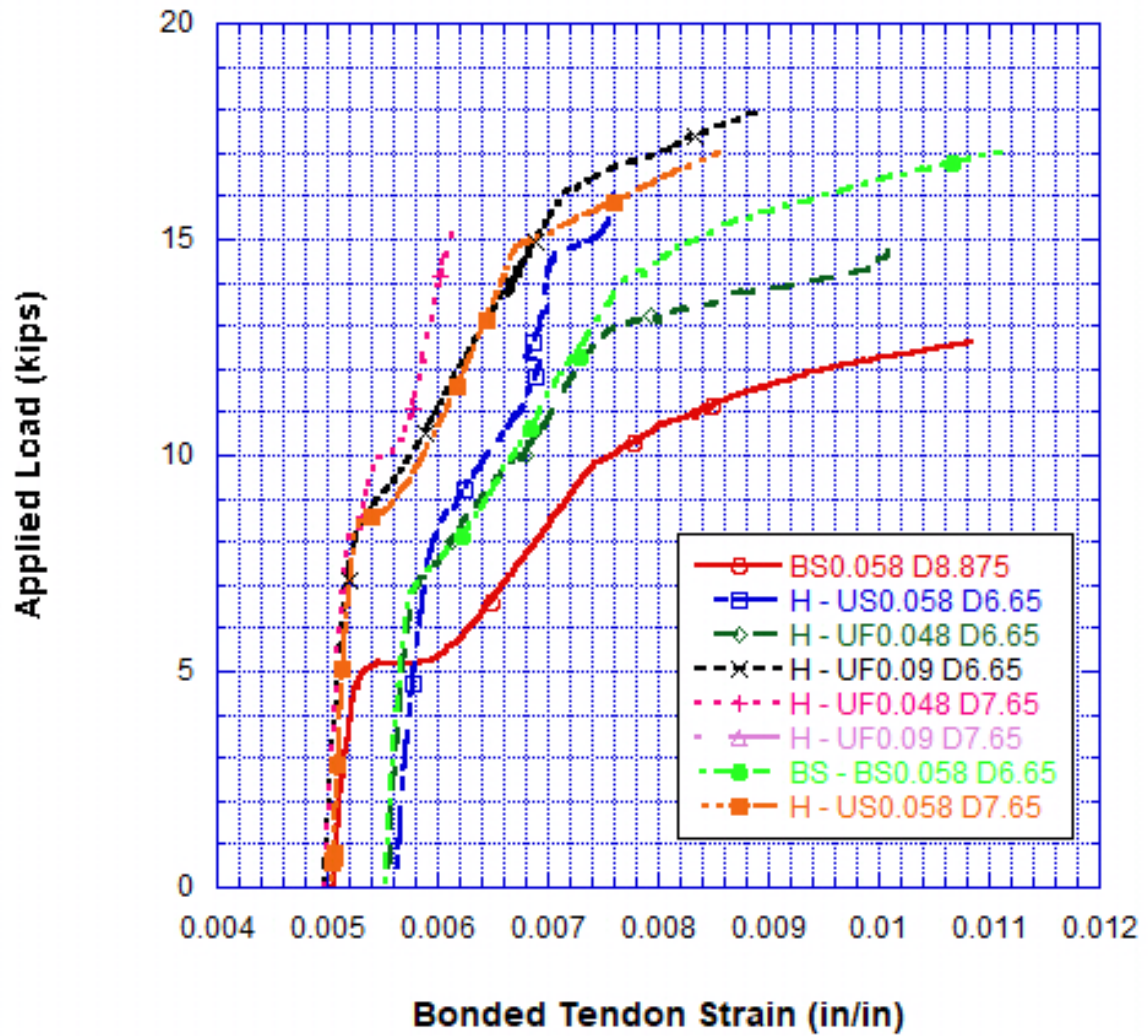


Figure 4.14 Load-strain behavior of the bonded tendon strain for all prestressed concrete beams tested

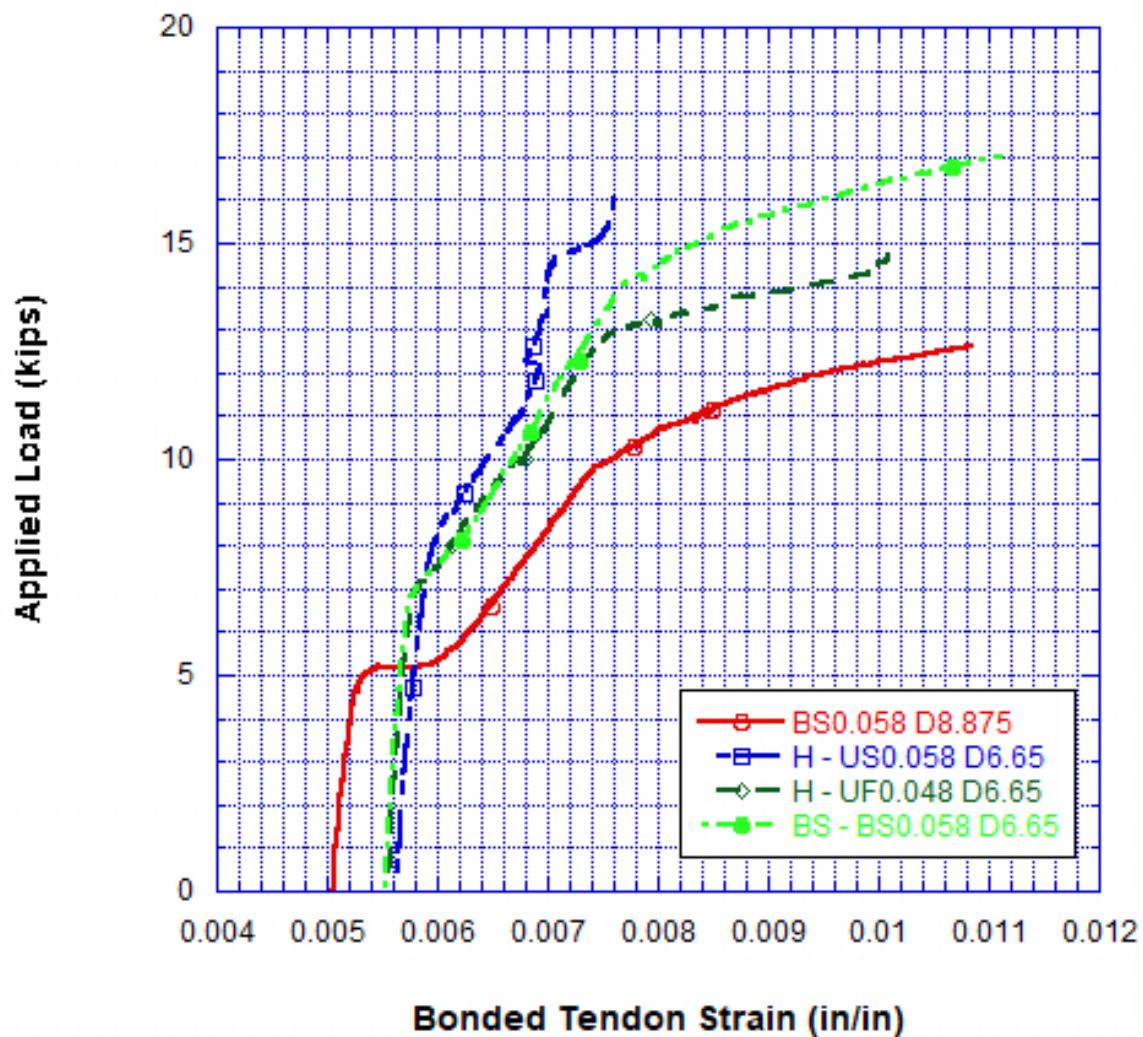


Figure 4.15 Load-strain behavior of the bonded tendon strain for the hybrid combination compared to fully bonded steel tendons

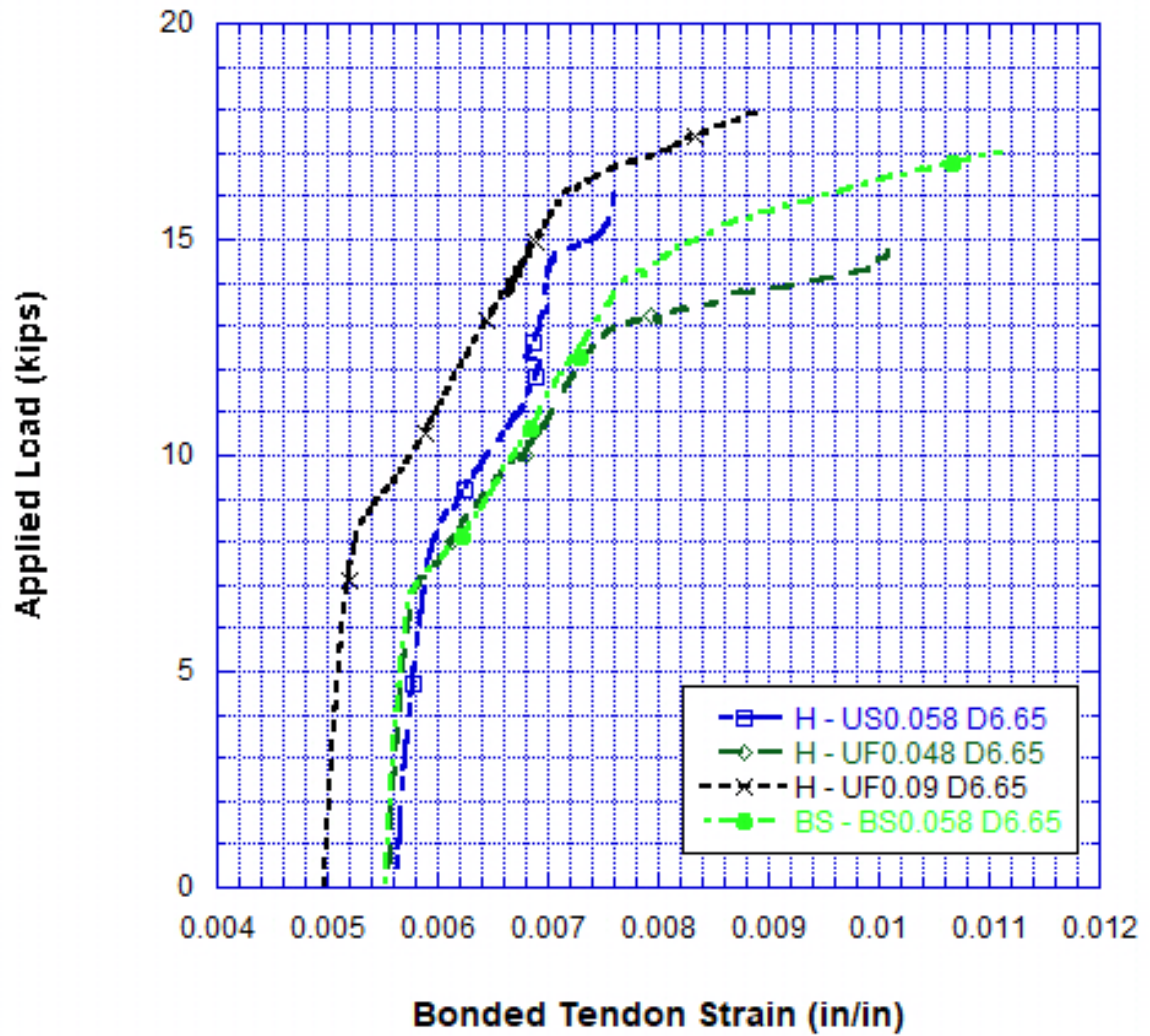


Figure 4.16 Effect of the area of the unbonded tendons at the same depth on the load-strain behavior of the bonded tendon strain



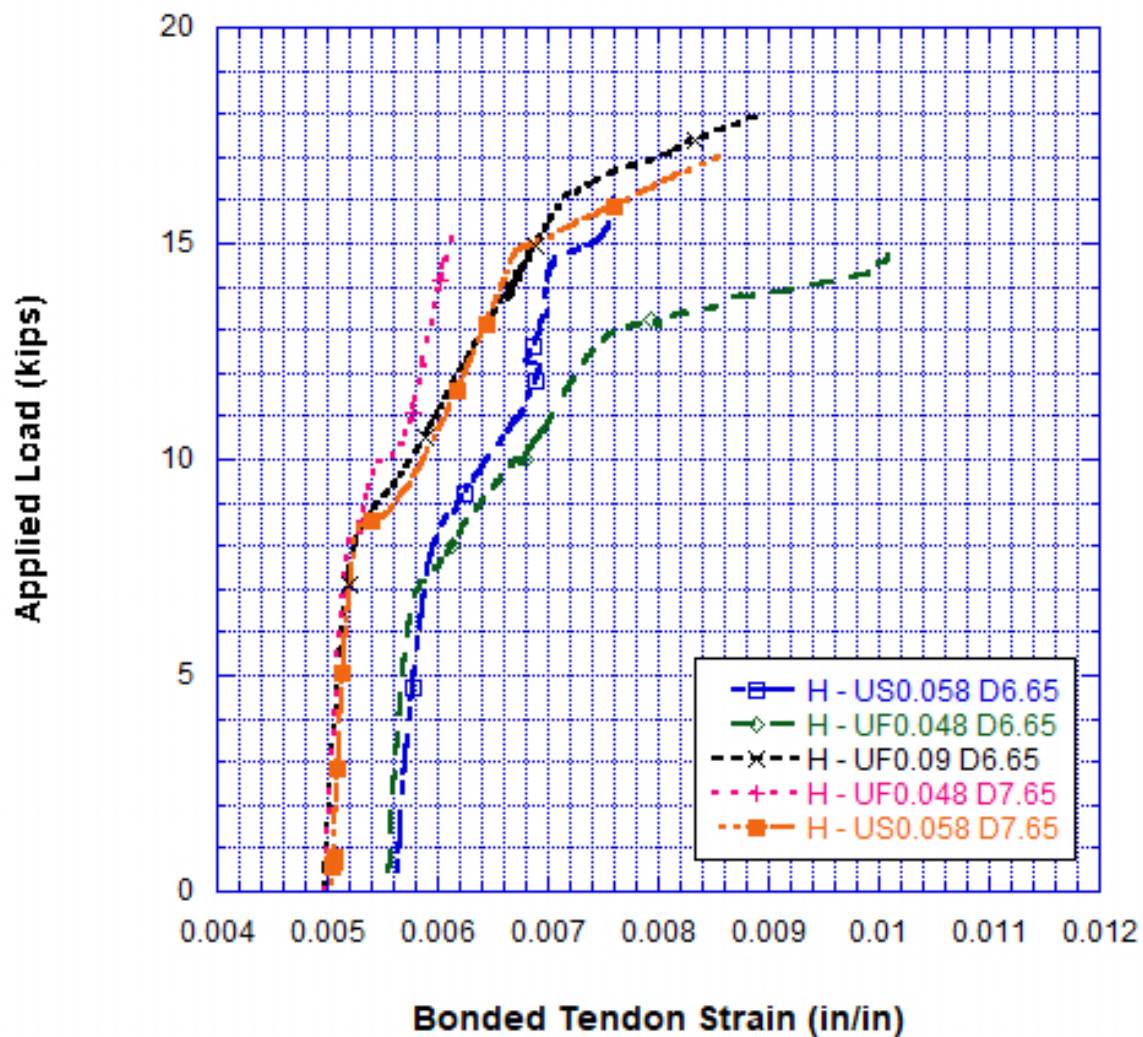


Figure 4.17 Effect of the unbonded tendons depth on the load-strain behavior of the bonded tendon strain

### 4.3.3 Stress and Strain in Prestressing Steel and CFRP Tendons

A 50 kip load cell was used to obtain the stress in the prestressed tendons. For all beams, the  $f_{pe}$  and  $f_{ps}$  were recorded and summarized in table 4.6. The unloading  $f_{ps}$  for beam H - UF<sub>0.09</sub>D<sub>6.65</sub> shows no reading because the CFRP tendon slipped during testing, so the data on the load cell after that point was not recorded. The effect of different parameters on the top tendons strain are shown in figures 4.18 – 4.21.

**Table 4.6 Summary of the effective stress and ultimate stress for the top tendons**

	Beam Designation	$f_{pi}$ (ksi)	$f_{pe}$ (ksi)	80-90% $f_{ps}$ (ksi)	Ultimate $f_{ps}$ (ksi)	Unloading $f_{ps}$ (ksi)
1	BS <sub>0.058</sub> D <sub>8.875</sub>	-	-	-	-	-
2	H - US <sub>0.058</sub> D <sub>6.65</sub>	175.9	173.8	213.9	249.1	219.8
3	H - UF <sub>0.048</sub> D <sub>6.65</sub>	195	192.9	229.7	320.9	257.9
4	H - UF <sub>0.09</sub> D <sub>6.65</sub>	208.2	202.5	226.7	296.9	-
5	H - UF <sub>0.048</sub> D <sub>7.65</sub>	214.9	207	274.0	317.2	243.1
6	H - UF <sub>0.09</sub> D <sub>7.65</sub>	201.1	205.4*	288.1	327.8	229.9
7	BS-BS <sub>0.058</sub> D <sub>6.65</sub>	189.5	186.2	269.4	288.4	283.2
8	H - US <sub>0.058</sub> D <sub>7.65</sub>	176.2	174.8	211.9	251.7	180.3

\*Grout was still being cured and gained more strength

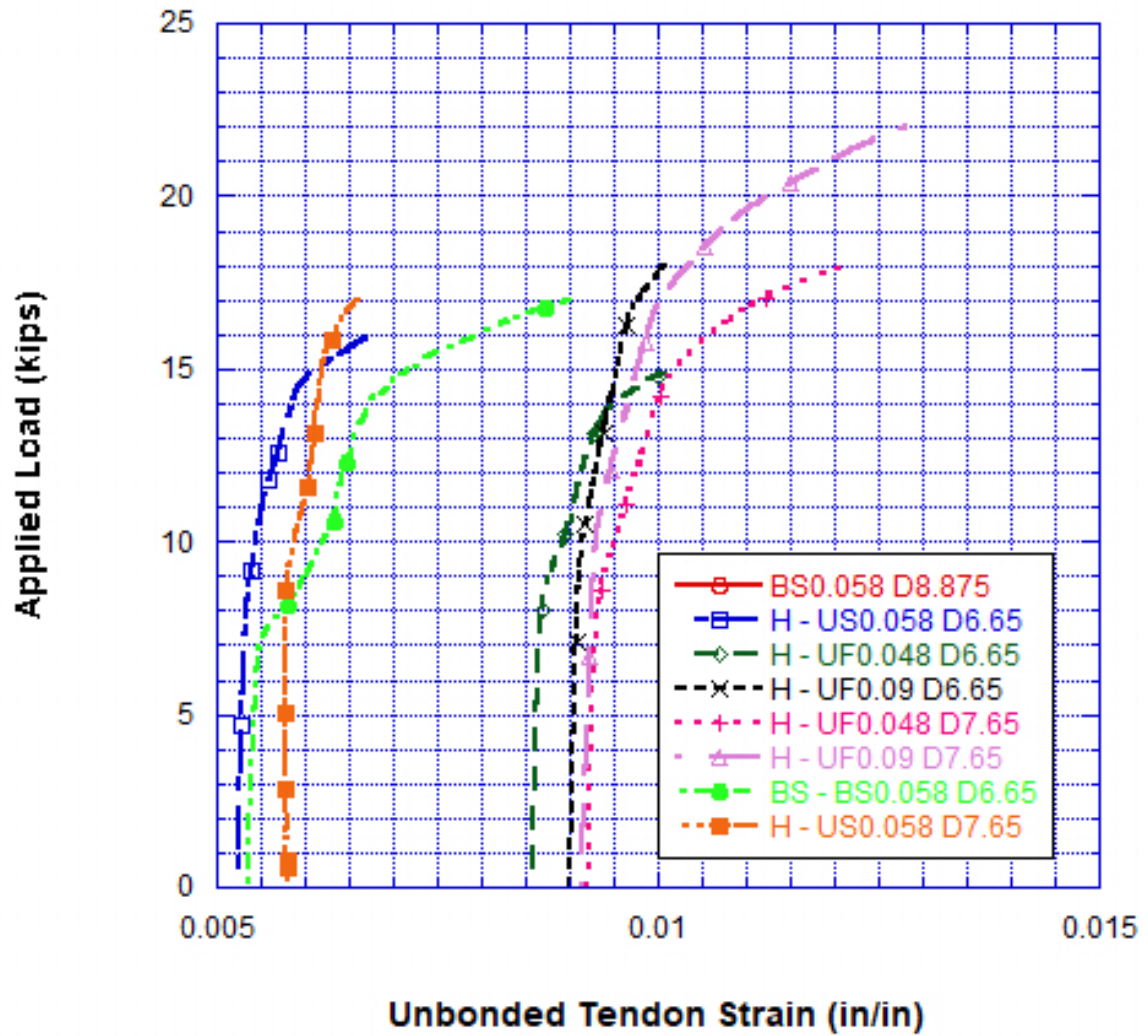


Figure 4.18 Load-strain behavior of the top tendon strain for all prestressed concrete beams tested



Figure 4.19 Load-strain behavior of the top tendon strain for the hybrid combination compared to fully bonded steel tendons





Figure 4.20 Effect of the area of the unbonded tendons at the same depth on the load-strain behavior of the top tendon strain

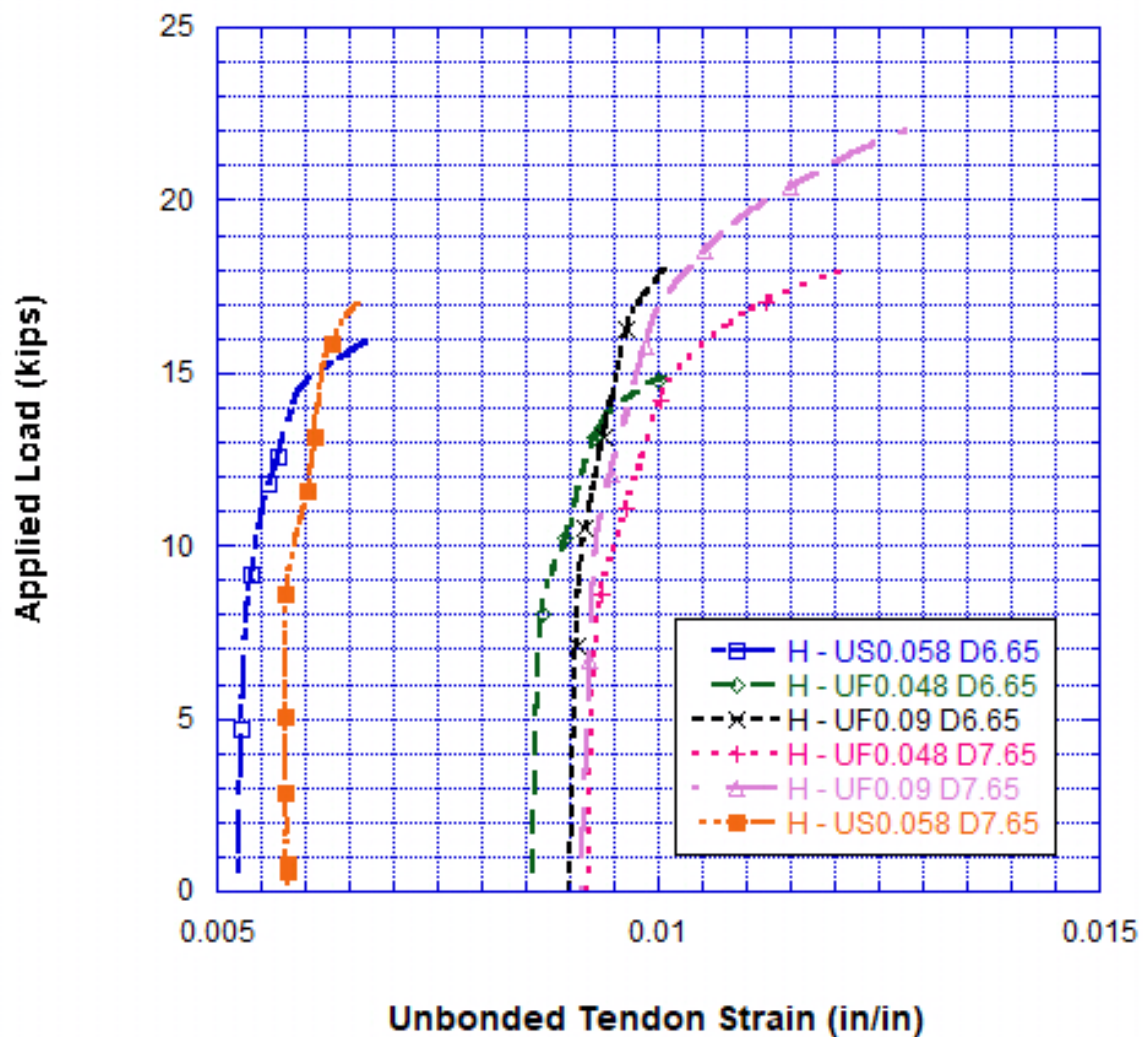


Figure 4.21 Effect of the unbonded tendons depth on the load-strain behavior of the top tendon strain

## **CHAPTER V**

### **5. MODELING AND ANALYSIS**

#### **5.1 Introduction**

In bonded tendons, the change in strain in the tendon is equal to the change in strain in the concrete section. However, in unbonded tendons, there is no strain compatibility due to the lack of bond with the tendon and concrete. The stress increase in the unbonded tendon depends on the member deformation. This demonstrates a challenge in producing an analytical model that can be applied at different load levels. The purpose of this section is to indicate the most accurate analytical model available that can calculate the ultimate stress in unbonded tendons used in hybrid beams.

#### **5.2 Trussed Beam Analogy**

##### **5.2.1 Finite Element Analysis (FEA)**

Figure 5.1 shows the trussed beam model demonstrating a prestressed concrete beam with a straight internal unbonded tendon. This model was presented by Tanchan (2001); Nassif and Ozkul (2002); Nassif, Ozkul and Harajli (2003); Nassif, Ozkul, Hwang and Han (2004); Ozkul (2007) and Unal (2011). The model was displayed as an idealization of a structural system divided into two key elements: the concrete beam element and the unbonded tendon element. Both elements are linked together at each end with rigid connectors and spring connectors throughout the full span of the beam. These springs are used to ensure deflection and curvature compatibility between the tendon and concrete beam. However, in the condition of hybrid beams with bonded and unbonded tendons, the bonded tendons are considered as rebar with initial stress condition. When

the beam is cracked, the tensile forces are shifted to the reinforcement. As deflection increases, the beam ends begin to rotate until the concrete fails in compression.

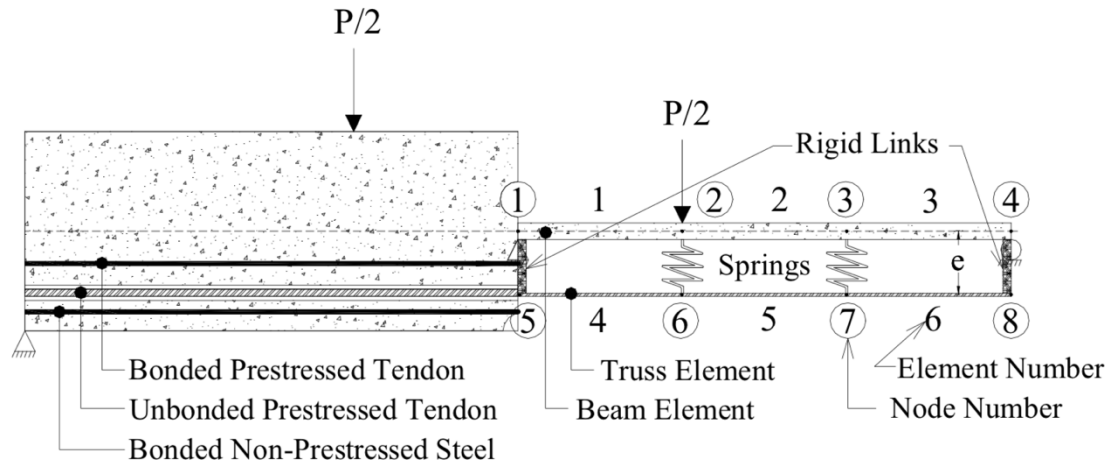


**Figure 5.1 Trussed Beam Model (Nassif, et al., 2003) (Unal, 2011)**

The trussed beam model was examined using a finite element program, ABAQUS (2016). This program includes numerous approaches to define certain material model and provisions for steel, CFRP, concrete, and boundary conditions. The model involves several factors listed below:

- A two-dimensional element demonstrating the concrete beam situated along its longitudinal axis.
- A truss element portraying the prestressing tendon.
- Springs connecting both the concrete and tendon elements.

The stress-strain relationship of several factors including concrete, steel, and CFRP, the bond slip between tendons, concrete, and reinforcing steel, and the failure criteria used have an effect on the accuracy of the finite element model.

Figure 5.2 shows the model for the concrete material which entails a compression and crack detection surface. The compression surface is an isotropically hardening yield surface which is active when the stress is mostly compressive. The crack detection surface determines if a point fails by cracking (ABAQUS, 2016).

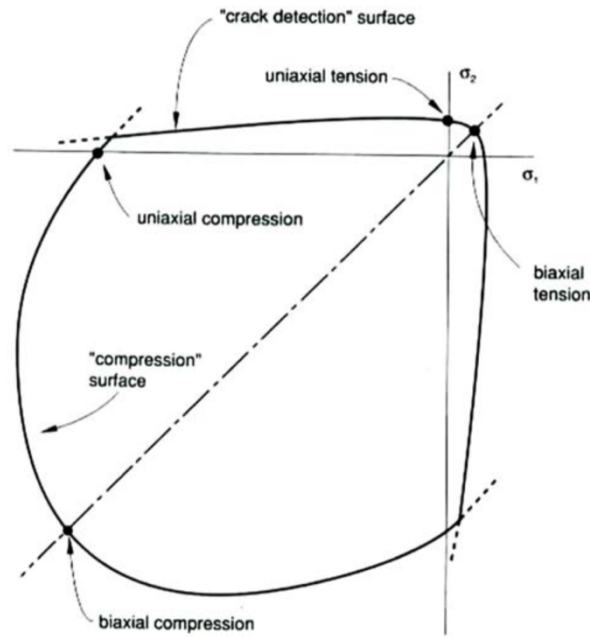
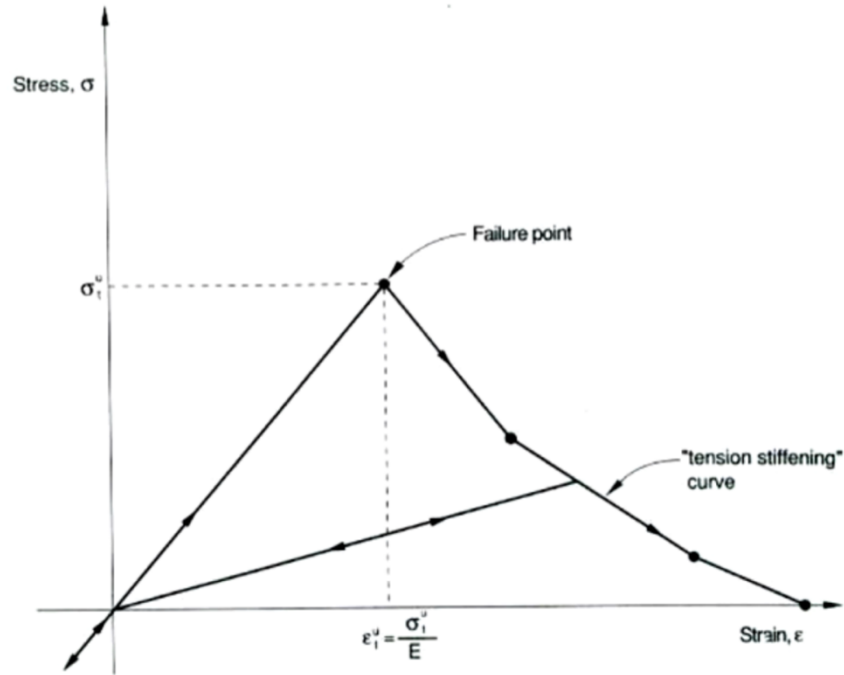


**Figure 5.2 Concrete Failure Surface in Plane Stress (ABAQUS, 2016)**

Concrete is predicted to reduce in strength through a softening mechanism and agree with a tension-stiffening model. Figure 5.3 shows a tension stiffening model that permits maintaining the stress that is not released when cracking occurs. When concrete reaches its ultimate tensile stress, the bond between the steel reinforcement and the

cracked concrete will allocate some tensile stress perpendicular to the cracked direction. The ultimate load and member deformation can be affected by different values of tension stiffening. The tension stiffening value is dependent on the reinforcing index, concrete bond, and reinforcing steel and tendon bond.

To determine the actual material stress-strain curves and failure points, the tendon and flexural steel reinforcement material properties are defined using the \*ELASTIC and \*PLASTIC commands (ABAQUS, 2016). The material properties are based on



experimental testing data presented in Chapter III.

**Figure 5.3 Tension Stiffening Model (ABAQUS, 2016)**

This experimental program will utilize the trussed beam model and apply it on the tested beams in this research to compare them with various code equations. This will be shown in Chapter VI.

## CHAPTER VI

### 6. COMPARISON OF RESULTS

#### 6.1 Introduction

The tested prestressed concrete beams in the experimental program are all modeled using the finite element software ABAQUS. The ultimate stress in the tendons ( $f_{ps}$ ), ultimate capacity ( $P_u$ ), and deflection are compared between the experimental results and the code equations.

##### 6.1.1 Comparison with the FEM Analysis

The comparison between the experimental results and the finite element modeling is shown in figure 6.1. The load deflection behavior of the modeled beams shows a similar behavior with the experimental results. Table 6.1 shows the difference in percentage in load and deflection between the finite element model and the experimental results.

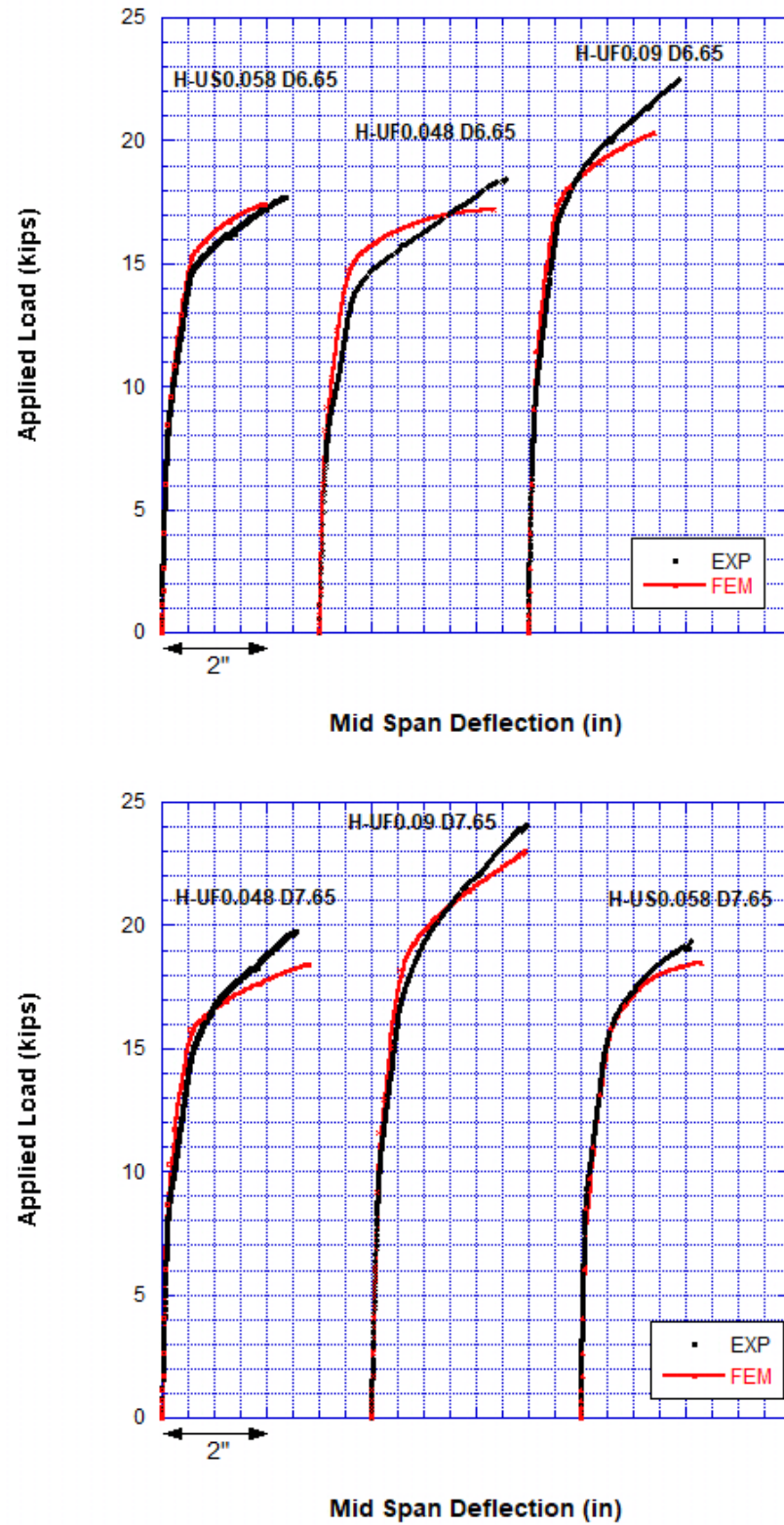


**Figure 6.1 Applied Load and Deflections Behavior for All Hybrid Beams:  
Experimental vs FEM**



**Table 6.1 Summary of the Load Deflection at Ultimate for Hybrid Beams  
(EXP vs FEM)**

Beam Designation	$P_u$ (EXP)	$\Delta_u$ (EXP)	$P_u$ (FEM)	$\Delta_u$ (FEM)	Percentage Difference %	
					$P_u$	$\Delta_u$
H-US <sub>0.058</sub> D <sub>6.65</sub>	17.71	2.36	17.40	1.95	-1.75%	-17.29%
H-UF <sub>0.048</sub> D <sub>6.65</sub>	18.46	3.58	17.19	3.34	-6.87%	-6.63%
H-UF <sub>0.09</sub> D <sub>6.65</sub>	22.49	2.88	20.30	2.39	-9.75%	-16.95%
H-UF <sub>0.048</sub> D <sub>7.65</sub>	19.77	2.58	18.41	2.80	-6.86%	+8.35%
H-UF <sub>0.09</sub> D <sub>7.65</sub>	24.09	2.96	22.98	2.93	-4.61%	-1.01%
H-US <sub>0.058</sub> D <sub>7.65</sub>	19.37	2.11	18.50	2.31	-4.51%	+9.50%

### 6.1.2 Comparison with the Design Codes

Many codes proposed equations to calculate the stress in the unbonded tendons, however, predicting the unbonded tendon stress in a hybrid member with bonded and unbonded tendons have not been adopted in the codes.

When using the proposed AASHTO (2017) equations on the experimentally tested beams, there was an average percentage difference of 16.3% for the hybrid beams. When using the suggested ACI 318-18 equation to calculate the unbonded tendon stress, there was an average percentage difference of 7.4% for the hybrid beams. Applying the suggested ACI 440.4R-04 equation to calculate the unbonded tendon stress, there was an average percentage difference of 34.6% for the hybrid beams. Results showed that AASHTO (2017) predicted equation underestimates the stress in the unbonded tendon and ACI 440.4R-04 tends to overestimate the unbonded tendon stress. A summary of the results are shown in table 6.2.

**Table 6.2 Summary of the Unbonded  $f_{ps}$  for Hybrid Beams (EXP vs Code Equations)**

Beam	$f_{ps}$ (ksi)						
	EXP	AASHTO	% Diff.	ACI 318	%	ACI 440	% Diff.
H-US <sub>0.058</sub> D <sub>6.65</sub>	249.10	219.27	-12.0%	272.72	9.5%	344.67	38.4%
H-UF <sub>0.048</sub> D <sub>6.65</sub>	320.90	239.53	-25.4%	325.17	1.3%	458.02	42.7%
H-UF <sub>0.09</sub> D <sub>6.65</sub>	296.90	247.10	-16.8%	286.76	-3.4%	292.68	-1.4%
H-UF <sub>0.048</sub> D <sub>7.65</sub>	317.20	260.82	17.8%	346.78	9.3%	387.83	22.3%
H-UF <sub>0.09</sub> D <sub>7.65</sub>	327.80	-	-	310.42	-5.3%	394.55	20.4%
H-US <sub>0.058</sub> D <sub>7.65</sub>	251.70	227.91	-9.5%	291.06	15.6%	459.39	82.5%
	Average:		16.3%		7.4%		34.6%

## CHAPTER VII

### 7. Conclusions

In summary, this study involved the testing of seven High Performance Concrete (HPC) beams with bonded and unbonded tendons using steel and CFRP tendons. Multiple variables included the area of the unbonded tendons, unbonded tendons material (CFRP or Steel), and depth of unbonded tendons. The testing results included the deflection at mid-span, ultimate load capacity, stress and strain in steel reinforcement, tendons, and concrete, crack numbers, width and spacing for all beams. Finite element modeling for all hybrid beam ultimate strength and deflections are discussed and compared to the experimental results. Comparisons of the ultimate stress (fps) in the tendons between the experimental results and the code equations were shown.

The following conclusions are presented from this experimental and analytical study:

1. Hybrid prestressed concrete beams show benefits in segmental bridge construction systems that could allow the use of CFRP as non-corrosive unbonded tendon material used in combination with bonded (steel or CFRP) strands.
2. The use of CFRP as an unbonded tendon in hybrid beams can maintain or increase the ductility of the member in terms of the number of cracks, their spacing and width if replaced steel tendons with the same diameter.
3. The FEA Trussed-Beam model solved using ABAQUS (2016) predicted a similar behavior of concrete beams prestressed with hybrid tendons.

4. AASHTO (2017), ACI 440.4R-04, and ACI 318-18 code equations do not predict the stress of the unbonded tendons in hybrid systems accurately when compared with the experimental results. However, AASHTO (2017) tends to be more conservative as compared to the other code equations.
5. There is a need to modify these Code equations to accommodate for the presence of hybrid tendons with bonded and unbonded combination of steel and FRP tendons.

## Bibliography

- AASHTO. "LRFD Bridge Design Specifications." *American Association of State Highway and Transportation Officials*. Washington, DC. 2017.
- ABAQUS Manuals, "User's Manuals – Version 5.8," *Hibbitt, Karlsson & Sorensen Inc*, Pawtucket, RI, 2016.
- Abu-Obeidah, Adi. *Flexural behavior of concrete beams prestressed with bonded and unbonded tendons*. Diss. Rutgers University-Graduate School-New Brunswick, 2017.
- ACI Committee 318. "Building Code Requirements for Structural Concrete." *American Concrete Institute*, 2018.
- ACI Committee 440.4R. "Prestressing Concrete Structures with FRP Tendons." *American Concrete Institute*, 2004.
- Beitelman, T. E. "Tensile test results of post tensioning cables from the midbay bridge." *Structures Research Center, Florida Department of Transportation*, <[http://ravenelbridge.net/post\\_tensioning\\_midbay\\_bridge.pdf](http://ravenelbridge.net/post_tensioning_midbay_bridge.pdf) (2000).
- Bennitz, Anders, et al. "Reinforced concrete T-beams externally prestressed with unbonded carbon fiber-reinforced polymer tendons." *ACI Structural Journal* 109.4 (2012): 521.
- Bondy, K. D. "Evaluation and repair of existing post-tensioned buildings with paper-wrapped tendons experiencing corrosion damage." *PTI Journal* 4.2 (2006): 24-29.
- Burningham, Clayton A., Chris P. Pantelides, and Lawrence D. Reaveley. "Repair of prestressed concrete beams with damaged steel tendons using post-tensioned carbon fiber-reinforced polymer rods." *ACI Structural Journal* 111.2 (2014): 387.
- Eamon, Christopher D., et al. "Life-cycle cost analysis of alternative reinforcement materials for bridge superstructures considering cost and maintenance uncertainties." *Journal of Materials in Civil Engineering* 24.4 (2012): 373-380.
- El Meski, Fatima, and Mohamed Harajli. "Flexural capacity of fiber-reinforced polymer strengthened unbonded post-tensioned members." *ACI Structural Journal* 111.2 (2014): 407.
- Ghallab, A., and A. W. Beeby. "Behaviour of PSC beams strengthened by unbonded Parafil ropes." *International Conference on Fiber-Reinforced Plastics for Reinforced Concrete Structures*. 2001.
- Ghallab, Ahmed. "Ductility of externally prestressed continuous concrete beams." *KSCE Journal of Civil Engineering* 18.2 (2014): 595-606.
- Grace, Nabil F., and George A. Sayed. "Ductility of prestressed bridges using CFRP strands." *Concrete International* 20.6 (1998): 25-30.
- Heo, S., S. Shin, and C. Lee. "Flexural behavior of concrete beams internally prestressed with unbonded carbon-fiber-reinforced polymer tendons." *Journal of Composites for Construction* 17.2 (2012): 167-175.
- Hussien, O. F., et al. "Behavior of bonded and unbonded prestressed normal and high strength concrete beams." *HBRC journal* 8.3 (2012): 239-251.
- Jerrett, C. V., S. H. Ahmad, and G. Scotti. "Behavior of prestressed concrete beams strengthened by external FRP post-tensioned tendons." *Proceedings of Advanced Composite Materials in Bridges and Structures*. 1996.

- Lou, Tiejiong, Sergio MR Lopes, and Adelino V. Lopes. "Nonlinear and time-dependent analysis of continuous unbonded prestressed concrete beams." *Computers & Structures* 119 (2013): 166-176.
- Naaman, Antoine E., et al. "Stresses in unbonded prestressing tendons at ultimate: Recommendation." *Structural Journal* 99.4 (2002): 518-529.
- Nanni, Antonio, et al. "Performance of FRP tendon-anchor systems for prestressed concrete structures." *PCI journal* 41.1 (1996): 34-44.
- Nassif, H. H., and Ozkul, O., "Flexural Behavior of Externally Prestressed Beams," Proceedings of the First Annual Concrete Bridge Conference, Nashville, Tennessee, October 6-9, 2002.
- Nassif, H., O. Ozkul, and M. H. Harajli. "Flexural behavior of beams prestressed with bonded and unbonded." *PTI Journal* 1.1 (2003): 60-71.
- Nassif, H., Eui-Seung Hwang, Ozgur Ozkul, and Man Yop Han. "Design and Analysis of Incrementally Prestressed Concrete (IPC) Girders." *The 2004 Concrete Bridge Conference Federal Highway Administration National Concrete Bridge Council American Concrete Institute (ACI)*. 2004.
- Nishizaki, Itaru, et al. "A case study of life cycle cost based on a real FRP bridge." *Third international conference on FRP composites in civil engineering (CICE 2006)*. Miami:[sn], 2006.
- Ozkul, Ozgur. *A new methodology for the analysis of concrete beams prestressed with unbonded tendons*. Vol. 69. No. 05. 2007.
- Ozkul, Ozgur, Nassif, H., Tanchen P., and M. H. Harajli. "Rational approach for predicting stress in beams with unbonded tendons." *ACI Structural Journal* 105.3 (2008): 338.
- Pham, T. M., T. D. Le, and H. Hao. "Behaviour of precast segmental concrete beams prestressed with CFRP tendons." *BEHAVIOUR* (2018).
- Roddenberry, Michelle, Primus Mtenga, and Kunal Joshi. *Investigation of carbon fiber composite cables (CFCC) in prestressed concrete piles*. No. BDK83-977-17. Florida. Dept. of Transportation, 2014.
- Schmidt, Jacob W., et al. "Development of mechanical anchor for CFRP tendons using integrated sleeve." *Journal of Composites for Construction* 14.4 (2010): 397-405.
- Shahrooz, Bahram M., Serpil Boy, and T. Michael Baseheart. "Flexural strengthening of four 76-year-old T-beams with various fiber-reinforced polymer systems: Testing and analysis." *Structural Journal* 99.5 (2002): 681-691.
- Taha, Mahmoud M. Reda, and Nigel G. Shrive. "New concrete anchors for carbon fiber-reinforced polymer post-tensioning tendons—part 1: state-of-the-art review/design." *Structural Journal* 100.1 (2003): 86-95.
- Tan, Kiang-Hwee, and Chee-Khoo Ng. "Effects of deviators and tendon configuration on behavior of externally prestressed beams." *Structural Journal* 94.1 (1997): 13-22.
- Tanchan, P., "Flexural Behavior of High Strength Concrete Beams Prestressed with Unbonded Tendons," PhD Thesis, Rutgers, The State University of NJ, New Brunswick, NJ, 2001.
- Thompson, Bill, and Mark Parlin. *Post-tensioned carbon fiber composite cable (CFCC), Little Pond Bridge, Route 302, Fryeburg, Maine*. No. 13-02. Maine. Dept. of Transportation, 2013.

- Zhang, Burong, and Brahim Benmokrane. "Design and evaluation of a new bond-type anchorage system for fiber reinforced polymer tendons." *Canadian Journal of Civil Engineering* 31.1 (2004): 14-26.
- Zhou, Wei, and Wenzhong Zheng. "Unbonded Tendon Stresses in Continuous Post-Tensioned Beams." *ACI Structural Journal* 111.3 (2014).